



Kaunas University of Technology
Mechanical Engineering and Design Faculty

Designing and Investigating of Electric Tricycle

Master's Final Degree Project

Vyom Chinubhai Shah
Project author

Prof. Dr. Kersys Arturas
Supervisor

Kaunas, 2018



Kaunas University of Technology
Mechanical Engineering and Design Faculty

Designing and Investigating of Electric Tricycle

Master's Final Degree Project
Vehicle Engineering (621E20001)

Vyom Chinubhai Shah
Project author

Prof. Dr. Kersys Arturas
Supervisor

Assoc. Prof. Dr. Vaidas Lukoševičius
Reviewer

Kaunas, 2018



Kaunas University of Technology
Mechanical engineering and design faculty
Vyom chinubhai shah

Designing and Investigating of Electric Tricycle

Declaration of Academic Integrity

I confirm that the final project of mine, Vyom chinubhai shah, on the topic “Designing and Investigating of Electric Tricycle” is written completely by myself; all the provided data and research results are correct and have been obtained honestly. None of the parts of this thesis have been plagiarised from any printed, Internet-based or otherwise recorded sources. All direct and indirect quotations from external resources are indicated in the list of references. No monetary funds (unless required by law) have been paid to anyone for any contribution to this project.

I fully and completely understand that any discovery of any manifestations/case/facts of dishonesty inevitably results in me incurring a penalty according to the procedure(s) effective at Kaunas University of Technology.

(name and surname filled in by hand)

(signature)



KAUNAS UNIVERSITY OF TECHNOLOGY

FACULTY OF MECHANICAL ENGINEERING AND DESIGN

Study programme VEHICLE ENGINEERING (621E20001)

**TASK ASSIGNMENT FOR FINAL DEGREE PROJECT OF
MASTER STUDIES**

Given to the student: Vyom Chinubhai Shah

1. Title of the Project

Design and Investigating of Electric Tricycle

Elektrinio triračio projektavimas ir tyrimas

2. Aim and Tasks of the Project

Aim. To design an Electrical Tricycle.

Tasks:

1. Problem Identification and providing alternative of typical vehicles: construction, powertrains and environment.
2. To create a model using CAD.
3. To analyze the frame of tricycle by FEM.
4. To make the prototype.

3. Consultants of the Project

Student:

(Name, Surname, Signature, data)

Supervisor.....

(Name, Surname, Signature, data)

Programme Director of the Study field *Janina Jablonskytė*

(Name, Surname, Signature, data)

Table of contents

Introduction	12
1.1. Surat city	12
1.2. Transportation in Surat.....	12
1.3. Vehicle Population	12
1.4. Introduction to Electric Tricycle	15
2. Literature review	16
3. Theoretical Background	21
3.1. History background of tricycle.....	21
3.2. Types of tricycle.....	21
3.2.1. Delta tricycle:.....	22
3.2.2. Tadpole tricycle:	22
3.2.3. Sidecar tricycle	23
3.3. Future aspects of Electrical Tricycle in India	23
4. Research methodology	25
4.1. Problem Identification.....	25
4.2. Electric Tricycle	26
4.2.1. Computer Aided Model	26
4.3. Material for frame	28
4.4. Boundary conditions of CAD model of Frame for FEA methodology.....	29
5. Calculations.....	31
5.1. Vehicle dimensions	31
5.2. Vehicle technical parameters	32
5.3. Vehicle drive scheme, gearbox gear ratios, final drive gear ratio.....	32
5.4. Vehicle tire dimensions.....	33
5.5. Vehicle dynamic characteristics: maximum speed, acceleration.....	35
5.5.1. The main vehicle's components arrangement in scheme (on lateral projection);	35

5.6.2 The main vehicle's components arrangement on coordinate axis x and z (data will be used for further calculations with "MAS1")	36
5.5.2. Vehicle element distance from the starting of the front tyre on coordinate system.	37
5.5.3. Comparison of calculated Centre of Gravity with SOLIDWORKS model.....	37
5.6. Theoretical calculations of vehicle gearbox.....	38
5.6.1. Theoretical gearbox transmission ratio calculations.....	40
5.7. The dynamics of the wheel	42
5.7.1. Wheel angular velocity	42
5.7.2. Wheel moment.....	42
5.7.3. Dynamic radius of the wheel	44
5.8. Forces acting on the vehicle;.....	44
5.8.1. The motor torque reserve.....	44
5.8.2. The power loss in the vehicle	45
5.9. Wheel rolling resistance force.....	47
5.10. Air resistance force	47
5.11. Vehicle pull (traction) analysis	50
5.12. Vehicle movement in the corner	52
5.13. A critical vehicle's rollover angle in the vertical longitudinal plane of the vehicle	55
5.14. Force calculation for frame FEA analysis.....	56
5.14.1. Bending Force.....	56
5.14.2. Torsion Force.....	56
5.15. Meshing Geometry for Analysis	56
6. Result and Discussion.....	58
6.1. Mesh result	58
6.2. Bending case	58
6.3. Torsion case	59
6.4. Lateral Case.....	60
6.5. Steering operational longitudinal load case	61
6.6. Natural Frequency.....	62
Conclusions	64
List of references.....	65

List of figures

Figure 1. Vehicle population with different categories [4]	13
Figure 2. Carbon Emission data for Surat city [3].....	14
Figure 3. Flyover as a source of parking space	14
Figure 4. Prototype of Electrical tricycle.....	15
Figure 5. Loading values on the frame [6]	16
Figure 6. CAD 3D drawing of hybrid tricycle [7].....	17
Figure 7. Concept design [9]	18
Figure 8. Collision Protection System [9]	19
Figure 9. First electric tricycle [14]	21
Figure 10. (a) Delta type, (b) Tadpole type	22
Figure 11. Sidecar Tricycle [17].....	23
Figure 12. Isometric view of Conceptual design of electrical tricycle.....	26
Figure 13. Frame of Tricycle	27
Figure 14. Boundary Conditions	30
Figure 15. Vehicle Projection and Dimensions	31
Figure 16. the arrangement of tricycle layout, i.e. rear wheel drive.....	33
Figure 17. Tyre parameters [25]	33
Figure 18. Tyre parameters [25].....	34
Figure 19. Tire speed index Numbers shows what maximum speed is allowed	35
Figure 20. Vehicle Component and user location layout	36
Figure 21. Data for C.G. Calculation.....	37
Figure 22. Result of Calculated C.G.....	37
Figure 23. Calculated C.G. in SOLIDWORKS.....	37
Figure 24. Comparison of C.G. calculated in SOLIDWORKS and by manual	38
Figure 25. Wheel rays.....	40
Figure 26. Basic construction of motor to wheel as powertrain [26]	40
Figure 27. Graph of wheel moment to wheel angular velocity	43
Figure 28. Vehicle kinematic speed to transmission power loss	46
Figure 29. Various drag co-efficient data according to vehicle categories [27].....	48
Figure 30. Frontal cross-sectional area of vehicle	49
Figure 31. Air resistance with reference to vehicle speed.....	50
Figure 32. dependence of vehicle kinematic speed on Vehicle pull force	52
Figure 33. Wheel base and steering turning angle α	52
Figure 34. Turning radius	53

Figure 35. Centrifugal force dependence on Vehicle movement speed	54
Figure 36. Critical vehicle's rollover angle [28]	55
Figure 37. Meshing properties.....	56
Figure 38. Mesh result	58
Figure 39. [a] Result of equivalent stress [b] Result of deformation in Y axis	58
Figure 40. [a] Factor of Safety calculation [b] Result of Fatigue life	59
Figure 41. [a] Result of shear stress [b] Result of deformation in y axis	59
Figure 42. [a] Safety factor [b] Result of fatigue life	60
Figure 43. [a] Equivalent stress on 50N [b] Total deformation on 50N force	61
Figure 44. [a] Equivalent stress [b] Total deformation	61
Figure 45. Natural frequencies	62

List of tables

Table 1. Vehicle Population [2].....	12
Table 2. Loading Cases	16
Table 3. Properties of Aluminum alloy [24].....	28
Table 4. Properties of Structural Steel [24]	28
Table 5. Notations for Forces and Fixture to the model.....	29
Table 6. Force application of Loading cases	30
Table 7. Electric Tricycle Dimensions.	31
Table 8. Technical Parameters	32
Table 9. Gear ratio	33
Table 10. Tyre parameters.....	35
Table 11. table Vehicle dynamic parameters.....	35
Table 12. Vehicle Elements with weight distribution and location.....	36
Table 13. Angular Velocity	42
Table 14. Wheel moment.....	43
Table 15. Vehicle kinematic speed and transmission power loss calculation.....	46
Table 16. Vehicle speed and Air resistance data	49
Table 17. Data calculation for 8 interval of RPM for $V_k(i)$, $P_t(i)$, $P_{oro}(i)$, $P_{in}(i)$	51
Table 18. Turning radius for different steering angles	53
Table 19. P_{is} calculated for four different values.....	54
Table 20. Load cases	56
Table 21. Max. deformation on each mode (remove deformation).....	63

Vyom Chinubhai Shah. Designing and Investigating of Electric Tricycle. Master's Final Degree Project. supervisor Prof. Dr. Kersys Arturas; Mechanical Engineering and Design Faculty, Kaunas University of Technology.

Study field and area (study field group): Transport Engineering (E12), Engineering Science

Keywords: Electric Tricycle, Computer Aided Design, Finite Element Analysis, Dynamics and Kinematics of Vehicle, Green Mobility.

Kaunas, 2018. 66 pages.

Summary

Surat city, Gujarat, India has a huge vehicle population over its area and human population. Moreover, two wheelers, including gasoline powered bikes and mopeds are leading category by population of 17 lakhs out of 22 lakhs hence, this category of vehicles is one of the biggest factor for noise and air pollution as they emit a huge amount of CO₂, CO, NO_x. Thus, Delta type Electrical tricycle is proposed as an alternative to replace gasoline powered two wheelers. Parts such as battery, motor, motor controller, wheels and braking systems are adopted from the electric bike and calculated for dynamic and kinematic conditions. Along with calculation, study carried forward to Computer Aided Design model of electrical tricycle is made with SOLIDWORKS. Furthermore, it has been imported and analysed by Finite Element Analysis method in ANSYS (v18.1). The FEA methodology included the tests of several loading case such as bending, torsion, lateral-braking operation, longitudinal-steering operation and natural frequencies. Succeeding with the satisfactory results gained with FEA method; Prototype (practical working model) was made and tested on the roads of the Surat City (Study Area).

Vyom Chinubhai Shah. Elektrinio triračio projektavimas ir tyrimas / Magistro baigiamasis projektas / vadovas prof. dr. Artūras Keršys; Kauno technologijos universitetas, Mechanikos inžinerijos ir dizaino fakultetas.

Studijų kryptis ir sritis (studijų krypties grupė): Transporto inžinerija (Inžinerijos mokslai).

Reikšminiai žodžiai: elektrinis triratis, kompiuterinis projektavimas, Baigtinių elementų analizė, automobilių kinematika ir dinamika, žaliasis mobilumas. Kaunas, 2018. Puslapių sk. 66 p.

Santrauka

Surato yra uostamiestis, Gudžarato valstijoje Indijoje, turintis didelį gyventojų ir transporto priemonių skaičių, o šioje valstijoje žmonių tankumas - net 2,89 mln. gyventojų (2005). Svarbu paminėti, jog čia populiarios dviratės priemonės, tokios kaip dviračiai, bei varomos benzinu - mopedai, benzininiai dviračiai, kurie yra pirmaujantys pagal kategoriją. Be to, dviračių transporto priemonių kiekis siekia nuo 170 tūkstančių iki 220 tūkstančių. Dėl to, ši transporto priemonių kategorija yra viena iš dažniausių priežasčių, sukeliančių triukšmą mieste.

Taip pat, transporto priemonės lemia oro užterštumo didėjimą žmonių gyvenamoje aplinkoje, kurių išmetamosios dujos turi didelį kiekį teršalų, tokių kaip CO, (anglies dvideginis) NOX dujos. Aktualu, kad dėl keliamų didelių užterštumo problemų, siūlomi Delta tipo elektriniai triračiai kaip alternatyva, pakeisianti benzinu varomas transporto priemones. Baterija, variklis, variklio valdymas, ratai ir stabdžių sistemos yra pritaikytos nuo elektrinio dviračio dizaino ir struktūros. Be to, šis modelis yra pamatuotas ir puikiai suprojektuotas įvertinant dinamines ir kinetines charakteristikas.

Svarstant apie realų projektą ateityje, tyrimas veda link tolimesnio projektavimo ir gilesnių ieškojimų. Kompiuterinės programos pagalba Computer-Aided Design(CAD) atliktas transporto priemonės dizaino kūrimo ir projektavimo darbas. Beje, elektrinio triračio modelio dizainas yra suprojektuotas su 3D modeliavimo SOLIDWORKS programa.

Be to, modelio veikimas ir duomenys buvo importuoti ir išanalizuoti pagal Finite Element Analysis metodą ANSYS (v18.1). FEA metodologijos bandymai apima kelis atvejus, tokius kaip: lenkimas, sukimas, šoninis stabdymas, išilginis vairavimas ir natūralūs dažniai.

Taigi, galima teigti, jog naudojant FEA metodą gauti teigiami rezultatai. Prototipas (praktinis darbo modelis) buvo sukurtas ir išbandytas Surato mieste (studijų erdvės) keliuose.

Introduction

1.1. Surat city

The transportation system in Surat city, India is taken as the area of study for the thesis. Surat is the city of Gujarat state situated in the western part of the country. Surat is the Economical capital of Gujarat state. Surat is 4th fastest growing city in the world. 8th largest city by population as well as area wise. Area of the municipal corporation of city is 326 square kms. Surat is known as a diamond city because governments statistics says that 9/10 diamonds in the world are cut and polished in Surat city. Surat city is also a big hub for textile market as India's 40% of man made fabric and 28% of man made fibers are produce here. Surat has a boon of Tapi river moreover Tapi river ends and meets to the Indian Ocean in Surat city. Thus, Surat a very long border touches to Indian ocean too which gives opportunities to developing ports and other industries as logistics connection to other countries are convenient here. L&T, Reliance, Essar, Adani ports, Shell, Gujarat State Petrol, Gail, ONGC and many more industries and companies are there in the city. The population of city is 4.6 million as Human population census 2011 which is assumed 6 million in 2017 and would be around 7 million in human population census 2021. The big industries attract more people to migrate in the city hence the migration ratio is too high, and it covers 56% of the total population of the city [1].

1.2. Transportation in Surat

The transportation system in the city is highly influences by continues increasing population and migration ratio. Two types of transportation systems are available in the Surat city. The first option is transport vehicles and the other one is Non-transport vehicles. Further Transport vehicles are being classified in two majors such as Goods vehicles and Passenger vehicles. Trucks/Lorries, three wheelers light goods vehicles and other light good vehicles are the sub categories of Good vehicles. Where buses, maxi, School buses, private service vehicles, Taxies, Auto Rikshaws are the part of Passenger vehicles. The category of Non-Transport Vehicles having sub categories of Police Van, Motor cars and station wagons, Jeeps, motor cycles, scooters, mopeds and tractors [2].

1.3. Vehicle Population

Table 1. Vehicle Population [2]

Year	Total Vehicle Population
2009-2010	1614340
2010-2011	1752118
2011-2012	1922382

Table 1 shows the numbers of vehicles are continuously increasing every year. Moreover, deep statistics of population of individual category bike population, car population and other transport vehicle population states the increasing ration of bikes and mopeds are highest even bikes and mopeds are the dominating transport means which leads the vehicle population since 2009 to 2018, even it could be judge that it will lead the vehicle population even in nearer future by the statistics shown in figure 1.

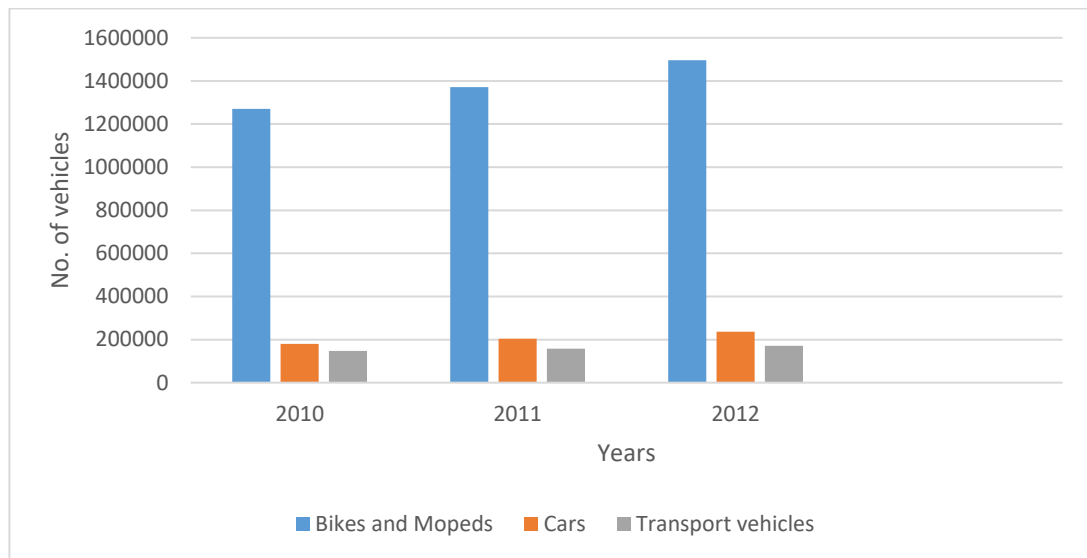


Figure 1. Vehicle population with different categories [4]

In the figure 1 population of vehicle is categorised in 3 types of transport means. Bikes and mopeds combined, cars include passenger cars, jeeps police vans. Trucks, lorries, tankers, all type of buses, private service vehicles, taxis, auto rickshaws and ambulance categorised by transport vehicles.

The statistical analyse of the vehicle population in Surat city has been predicted 26 lakhs by the Times of India in 2013 [2]. It is calculated that 13.52 percentage of vehicles are increased during the duration of three years in 2012 to 2015. By the calculation it could be predict that the population of the vehicles in the Surat city in 2018 is almost 30 lakhs.

The number of transport vehicle was 170716 in 2012. In year of 2015, RTO Surat has published the vehicle population statistics. That shows number of registered vehicle is around 22 lakhs in 2015 where the population is about 4.6 million as per census 2011[2]. In this statement it is mentioned that population of Motorcycles and mopeds is 17 lakhs in Surat city in the year of 2015.

Here the Motor cycles and mopeds population increasing percentage shows that people use it more than any other transport mode. The petrol-based motor cycles and mopeds are one of the major source of the air pollution by emitting Co, CO₂, NO_x gases in the environment. Moreover, they are a big

factor of traffic issues in the city. Total Carbon emission of the city includes residential, commercial, industrial, transport and wastes. In these categories highest carbon emitting parameter is industrial however; transportation system is second leading parameter which has 33% of total carbon emission. The % sharing for carbon emission for these parameters are shown in figure 2.

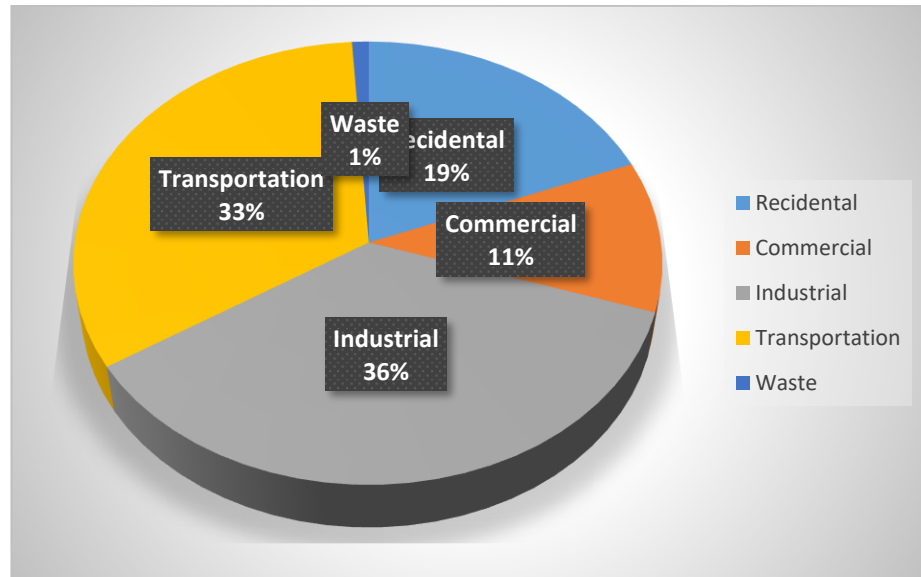


Figure 2. Carbon Emission data for Surat city [3]

All cited categories are actively contributing to 3.38 million CO₂ annually. Carbon emission was 0.921 Tones per year in year of 2007-2008 from that corporation level emissions were about 3.50% approximately. Transportation is 2nd leading factor by 33% in that highest is bikes and mopeds [5].

Finding the alternative solution for this individual is the burning issue in the city. Surat Municipal Corporation is however working for this. There are 98 flyovers and bridges which is 2nd highest in India, more 15 bridges are under construction. All of them are allowed for all type of vehicle including heavy loaded trucks with 20 tonnes of dynamic load [3].



Figure 3. Flyover as a source of parking space

Fly over is not only the solution for providing better road but it is also being a good source of parking too.

Also, they have taken actions such as increasing the frequencies of city buses B.R.T.S. buses, expansion of the roots of city buses and B.R.T.S. buses, decreasing the fare of traveling by buses, providing more facilities in buses like Wi-Fi, e-tickets, urban bus stations. Though the use of private bikes doesn't decrease; the reason is adopted by the local survey done. It is to be said that bikes are more convenient for short distance and some areas where buses can't reach. For travelling few of areas of small streets and underdeveloped area bikes are less time consuming where people who travelling by bus must walk and its time consuming. Also, buses are not convenient for old age people and handicaps as walking is obstacle for them. According to such reasons elimination of petrol bikes completely is not possible. Hence, finding an alternative solution is needed.

1.4. Introduction to Electric Tricycle

As a Sustainable green mobility transport mean, electrical tricycle is to be proposed for the Non-transport vehicle category where there were only motorbikes and mopeds are the options in existing format of non-transport vehicles.

Electrical tricycle could have 2 types of designs: tadpole or delta. Here, I am proposing the design of delta type of electrical tricycle which means single front wheel and two rear wheels.



Figure 4. Prototype of Electrical tricycle

2. Literature review

A. Rodríguez, B. Chiné and J. A. Ramírez made an electric tricycle frame model with Solidworks CAD modeling. Further model imported to the Comsol Multiphysics, then the Structural Mechanics Module is used to define two different 3D FEM models, the beam structure and solid mechanics were selected for the analysis. Aluminum 6063-T83 material applied on most of the parts of the frame where bottom bracket and handlebars are made of steel 4130. The reason of choosing steel 4130 wasn't specified however it is understood by the properties of the material and function of the component. Bottom bracket and handlebars have to perform with heavy load compare to other parts of the chassis. Steel 4130 has significant more yield strength compared to Aluminium 6063-T83 thus it was applied according to the application.

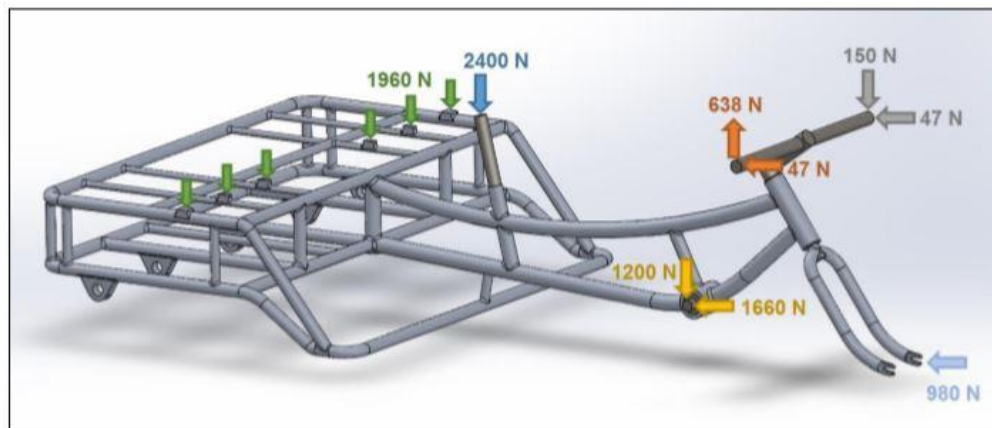


Figure 5. Loading values on the frame [6]

All loads acts on the frame is shown in the figure 5 however all of them do not acts on each case, the analysis of the frame is done for 3 particular cases are Acceleration, steady peddling and Horizontal impact.

Table 2. Loading Cases

Loading cases	■	■	■	■	■	■
1. Acceleration		✓	✓	✓		✓
2. Steady Pedalling					✓	✓
3. Horizontal Impact	✓					✓

As shown in table 2 five loads acts on the case of acceleration that are on both side of steering, pedals, driver and passenger seat area. In case of steady pedalling loads acting on driver's seat position and passenger's seat position. While horizontal impact loads acts on the passenger's seat and steering rack. As a resultant some areas of the frame suffers from stresses even more than tensile yield strength

of 214 MPa are mostly all joints and other small pipes in the rear section of the frame which is for passenger and driver seat and hence it is stated by the author that there is a need of fine tune the frame geometry. Mover, fatigue and impact simulation has been suggested by the author which could be only done after all part became enough strong to withstand working stresses acting on the frame which shouldn't go above on yield strength of 214 MPa [6].

To provide an alternative solution of auto rickshaw, manual human power tricycle is made with hybrid electric and mechanical powered system by P.P. Dutta and S. Sharma. It is made to overcome the issue of environment pollution the other objective is to provide better ergonomics so that handicaps and old people also can ride it. Dutta and Shama took standard parts from bicycle and tricycle available in market which includes chain drive, wheels, freewheel and axle. Frame as a base structure of the rickshaw was made with mild steel pipe of 25 mm diameter.



Figure 6. CAD 3D drawing of hybrid tricycle [7]

The construction of the vehicle is shown in figure 6. The vehicle has two seats both persons has mechanical paddle to operate the tricycle where the steering handle is only one with single hand operator mechanism. Two different types of analysis performed on the vehicle are stress- deformation and safety test with objective of load bearing capacity and safety and aerodynamic analysis which has objective of minimum air drag. During the front impact test 9.44487×10^7 Pa of max. stress is felt on the frame and the min. Stress felt is 0.00092 Pa. Other tests include rear impact test, front bumper test, rear bumper tests and roll over test also performed on the frame model with Ansys software. Roll over test was performed with limitation of deformation and just to show the importance of the central antiroll bar, else the test result isn't shows the values of stresses or deformation. The vehicle made for old age people and handicap people too. It has speed limitations and charging range limitation too. [7]

Central Mechanical Engineering Research Institute, Kolkata had researched and made an electrical tricycle to replace IC engine powered auto rickshaws. The prototype made with solar powered charging system too. In the suspension system 1 shock absorber was provided to reduce the shocks and headlight was given for comfortable riding in night time. Which could be also helpful in fog or rainy atmosphere for better visibility. Moreover, rear wheels were manually powered and also could be run on the motor power. The total load carrying capacity was 200 Kg and max. speed of the vehicle was 15 km/h [8].

Swarnim Shrishti and Anand Amrit made a tadpole type hybrid tricycle with adjustable seat for rider and roof for sun protection with objective of weight reduction, improvement in durability, aesthetics and aerodynamic efficiency, to develop and efficient energy storage system and roll over protection system. Here, riders comfort was the focus for the modeling of the vehicle thus seat was made adjustable according to the height.

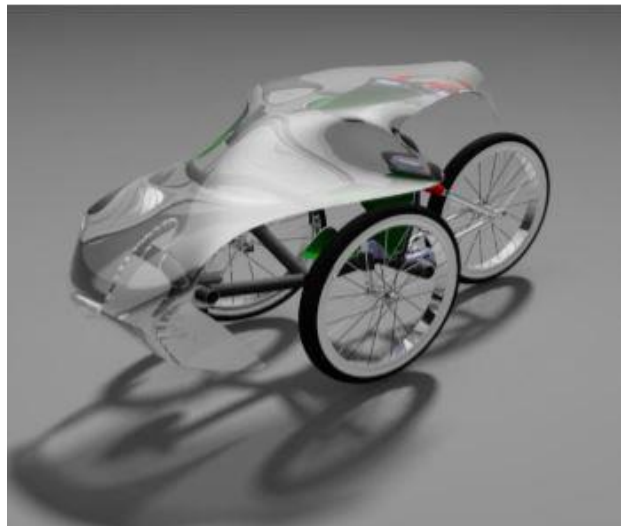


Figure 7. Concept design [9]

Model shown in figure 7 is final design which has three wheels in that two are in front a single wheel on back side so called tadpole type tricycle. Rest of other common research area the model has a good aerodynamic roof to reduce air drag. Design of aerodynamic roof made with Catia V5 software and imported to the Ansys Fluent for the Computational Fluid dynamics analysis. The CFD analysis done with the frontal area on which Air touches the vehicle body. The coefficient of drag value is derived 0.009, thus it gives a stable ride in particular direction.

Roof has a huge influence on the driver's visibility angle and such research is missing in the study. However seat is adjustable, so achieving a good visibility angle by adjusting seat is possible. Collision Protection system is another advantage of the vehicle which acts as a active safety system in the vehicle by applying brake by sensing other vehicle or any big object in critical near area of

the vehicle. This system has disadvantage of requirement of high torque motor for application of braking before collision.

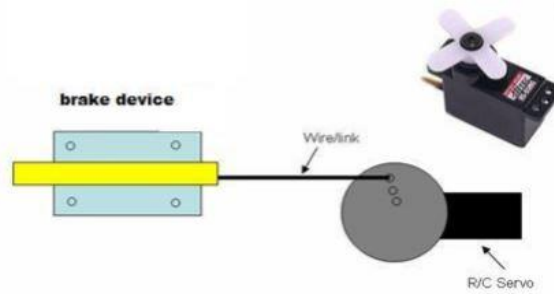


Figure 8. Collision Protection System [9]

On the addition of Collision prevention system, the tricycle has regenerative braking system to save some amount of energy while braking operation. The regenerative braking system has two dynamometers one in front side between both front wheels and other one is in the rear wheel which could produce 12V electric current. The system is clamping down on the wheel rim. While applying the brake, rubberized wheel comes in contact with rim, and spin the shaft connected to electric motor and generating electric current. Such electric current then stored in 12v battery and could be useful to provide electric power to perform any electrical operation. The frame of the vehicle is made with Aluminium 6061-T6. For material selection Stainless steel AISI 304 and Aluminium 6061-T6 were compared. A static structural test proven that stainless still material is more suitable than aluminium for such frame structure of model. Frame model made with Solid works and analysed in Ansys for several conditions and tests. Frame was tested for two different load conditions, a 2722N on top at 12° from vertical and a 1361N side load. The result for top loading condition is 16.31mm here 1.4mm deflection occurs in side loading. Both the load case resultant stress was also found below yield strength and predicted the design is safe. The critics of the vehicle is implementing the regenerative braking system and collision protection control system could increase the price as well as weight. Regenerative braking system could be justified by analysis of number of braking and calculation of quantity of electricity produced [9].

Prof. S. U. Gunjal, Prof. G. D. Sonawane, Prof. S. P. Awate and Prof. D. R. Satpute had a project of electrical tricycle as to provide a non-pollution creative vehicle as environment pollution is increasing vastly, the model of hybrid electrical tricycle is made for short distance travelling. The design of vehicle is ultra light and could be powered by human or electric power by batter so called hybrid vehicle. Vehicle adopts bicycle parts and electrical components from other electrical vehicles. The vehicle has two seats and could be drive manually by human power with both passenger's efforts and could be drive with electrical power supplies from battery. The steering of the vehicle is adopted from the bicycle and operated by one person only. Total length of vehicle is 2270 mm which is so high

compared to other tricycle length of 1800-200 mm. Also, turning radius is 3.3m with 45° steering turning angle, PMD motor of 1500 rpm and 48volts. Here, turning radius is mentioned in assumed dimension without calculation, such calculation and calculation of Centre of gravity of the vehicle are required for the dynamic stability of the vehicle. Frame of the vehicle has been made by CAD software and also been analysed by FEM analysis in ANSYS software. The material selected for all frame structure is aluminum Alloy T6. Structural analysis is done by applying load of 1128 N on drivers position and 200 N on paddle's position. However, 1128N is being calculated from weight of 115 Kg weight of driver but it not mentioned that it is for each or combined. If combined then it must have applied in combination on both the position, if it singular then another 1128 N force is needed which not existing in the analysis, but the result of the analysis says 25.64 N/mm² is the max. von misses stress where 0.9983 mm deflection occurs. Shock analysis done with 3G load is equivalent to loading force of 6900 N on single front wheel for this frame. Von misses stress 64.622 N/mm² felt by the body and Deflection is came 4.197mm. The frame is checked for rollover impact with 5000N on one side and said to be critical load for the frame. The Von misses stress felt by the frame structure is 119.429 N/mm² and Deflection occurred in the body is 8.603mm. The yield strength of material is 275 MPa thus design is said to be safe for all this tested case [10].

All above literature has one common objective to make a non-polluted vehicle to replace IC engine vehicles that exhausts Co, Co₂ ad NOX in high rate, as reducing the pollution from transportation system is highly needed. Such objective is achieved by the electric vehicle but adopting electric vehicle instead of gasoline powered vehicle by people is still a big challenge. All of the cited literature has an analysis of frame structure and most of them have proven with CAD modelling and FEM analysis the frame is enough strong to withstand all working loads. The other objective is to provide enough ergonomics for the rider. In hybrid system with human power by paddling human efforts is required to drive which leads to human energy loss and rider could become tired for big distance. The tadpole tricycle design has rack and pinion steering mechanism which increases weight and also complicates the designing which differs in delta type tricycle by simple mechanism of rack and stem with handlebars like motorbikes and bicycle.

3. Theoretical Background

3.1. History background of tricycle

First electric vehicle was invented by various people, but small model of electric car was made by a Hungarian guy Anyos Jedlik who invented an early type of electric motor in year of 1834 [11]. Thomas Davenport had built same prototype which was operated on the small circular electrified track [12]. Professor Sibrandus Stratingh of Groningen also had made a small type of electric car which run on non-chargeable primary cells [13].

The first electric tricycle was made by Englishmen William Ayrton & John Perry of England in year of 1881, which had two rear wheel and single front wheel. Front wheel was smaller compared to rear wheels and the right wheel was a driving wheel and other both were driven wheel. Front wheel was connected with the steering. It was so called as electrical wheelchair.

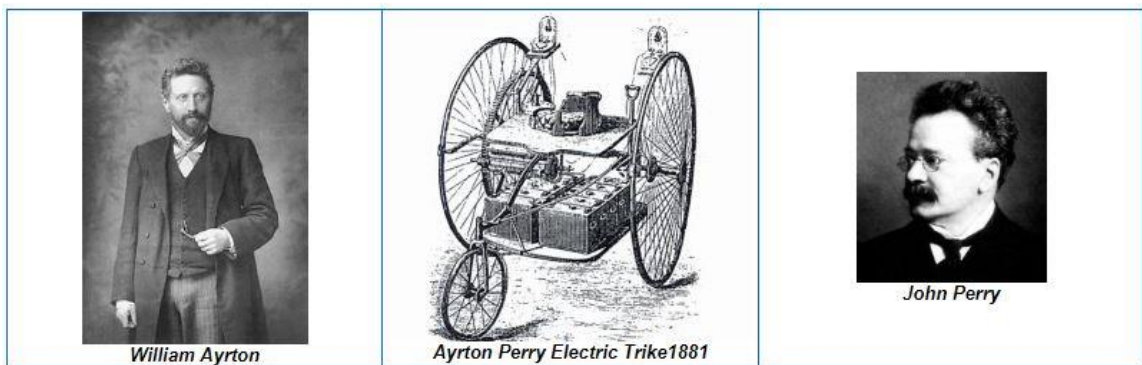


Figure 9. First electric tricycle [14]

The model had a lead acid battery of 10 cells connected in series producing $\frac{1}{2}$ horse power. Maximum speed of the vehicle was 14 km/h and riding range was 16 kms to 40 kms. The vehicle was 1st vehicle which contained electric light. In the year of 1882 rechargeable batteries invented by company named Elwell-Parker Ltd. Those batteries were used in passenger carrying trams around Birmingham, England in year 1890 [14].

3.2. Types of tricycle

There are three main types of tricycles.

- Delta tricycle
- Tadpole tricycle
- Sidecar tricycle

Tricycle is defined by its wheel arrangement. Above cited types of tricycles are most common. Delta tricycle has single front wheel and two rear wheels. Tadpole tricycle has single rear wheel and two front wheels. Sidecar tricycle has two wheels inline with each other and one wheel is parallel and offset.

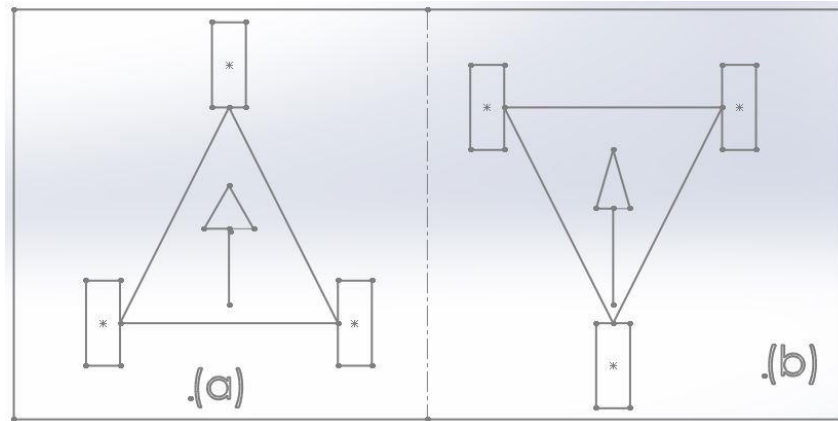


Figure 10. (a) Delta type, (b) Tadpole type

3.2.1. Delta tricycle:

Delta tricycle is also referred as traditional or rear load tricycle which simply means cargo or passengers position at rear side. The steering system is front wheeled as same as bicycle and battery compartment is also situated in rear side of the vehicle, thus C.G. is stays in rear side. Stability of the vehicle is much higher on low speed [16]. Dynamic behaviour of Delta tricycle includes braking operation and turning operation. In braking operation vehicle could stop by applying 1G braking force as the C.G. stays after forward axis. Thus, braking operation in slow speed could easily and efficiently done with 1G force. Conversely, driving of the vehicle on uneven steep grade surface chances of vehicle lifting from front side is more as the C.G. located in rear side. Turning operation is also stable in low speed as C.G. is well placed in rear side. However, height of C.G. is bit higher so long wheel base needed for the better stability and it helps to decreases twitchiness steering and improve the steering controlling even in high speed.

3.2.2. Tadpole tricycle:

Tadpole is having two wheels in front and also the passenger or cargo weight is also there in front of the driver seat. The Ackerman steering system could be use for tadpole tricycle because two wheels needed to steer hence it is more complicated and heavier than Delta tricycle [15]. Dynamic behaviour includes braking operation and turning operation, both depends on C.G. In the case of tadpole tricycle C.G. located in front side of the vehicle. While braking on 1G force vehicle stops generally, but in the case of high speed or downward inclination of hill chances of lifting of rear wheel is more while

braking operation. C.G. in front side creates un-stability even in turning by increasing the wheelbase it could be solve but turning radius will increases also on the downhill driver's visibility angle will be decreases.

3.2.3. Sidecar tricycle

Two wheels are inline like bicycle and one wheel is parallel and offset from the centre line. Mostly it is made for handicaps people. The arrangement of third wheel is in offset of the centre line of both other wheel.

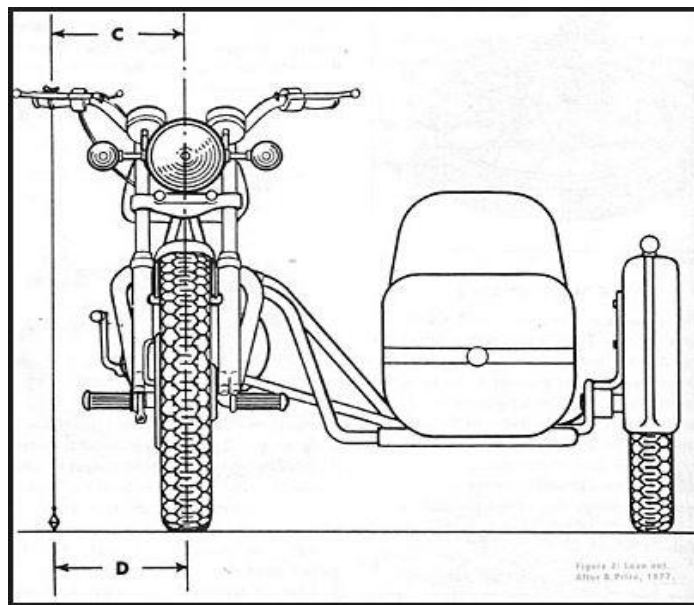


Figure 11. Sidecar Tricycle [17]

It also contains the same steering as bicycle but here, dynamic stability of the vehicle is challenge as there would be a big structured frame for passengers may creates the design heavier and C.G. varies according to the extra compartment size and location [16].

3.3. Future aspects of Electrical Tricycle in India

In India, research on Electric vehicle is going in all automotive R&D institutes, also academic and industrial institution are bringing motivated to research and development in field of electric vehicles. Moreover, Indian government is promoting Electric vehicle on a large scale too. Government is planning to give 14,000 Crore INR subsidies to Electric Vehicle Manufacturer and this is how government of India could save 30,000 Crore INR of fuel from fuel-based vehicles. Also, target has been fixed by Indian government to produce 6 million electric vehicles as green mobility vehicle till 2020. From that approximately 4 to 5 million would be two wheelers. As of now, there are only few electric vehicles are existing in that around 4 lakhs are two wheelers and 1500 four wheelers [18].

In the place of 4-5 lakhs of electric two wheelers, electric three wheelers could be proposed for special purposes i.e. for old age people, for handicaps who has disabilities in legs, for people who are interested in innovation and are ready to adopt new technology.

There is no driving licence needed for electric vehicles having motor of 250V or less. However, helmet is required even for vehicle having motor capacity of 250V, more or less. For the electric cars, driving licence must required. Charging station operator doesn't need licence for providing charging stations to charge electric vehicles as it doesn't come under the act of electricity 2003, as it is not transmission or distribution or trading of electricity [19].

4. Research methodology

The electrical Tricycle is designed and modeled with Computer Aided Designing software and analysed by Finite Element Analysis methods. The objectives of the research work include:

- To provide sustainable green mobility vehicle
- To reduce noise and environmental pollution
- To provide an alternative of IC engine two wheelers
- To provide most comfortable, safe and easy transport mode for all age group
- To provide option instead of wheel chair to the production vehicle to handicap people with having disabilities in legs

4.1. Problem Identification

By the statistics of the vehicle population and pollution by vehicles, need of alternative option for IC engine vehicles is stated [4]. Number of two wheelers are most in compare to all other categories of the vehicles in India and especially in Surat City which has been chosen as an area of study leads to find replacement option for fuel powered two-wheeler vehicles.

Electrical energy usage for vehicle is been selected as it is non-polluted energy source for vehicle. Whereas other fuels are fully or partially pollution generated vehicles. The most populated vehicle category is two-wheeler vehicles. The need of using two wheelers are most important to understand. The sports bikes and bikes having engine capacity of 100 cc or more are use as a bike riding hobby of people which can not be replace by electric vehicle. However, the bikes and mopeds of engine capacity of less than 100 cc are purely used as a small or medium transportation around city for one or two persons. Moreover, the speed limit for bikes and mopeds in city is varies by road to road is 40-50 km/h [20]. This segment of vehicles is most used by the people of Surat city as per the RTO Surat [21]. By finding the alternative of this particulars, issues of pollution could be partially solved, and other objectives could be achieved.

This two-wheeler segment is compared with three wheelers. While comparing the both tricycle has more stability, easy to operate, even no driving licence needed, all age group people can drive, better safety, self balanced vehicles and more comfort than bikes even for more frequent travels per day hence, Electrical Tricycle has been proposed.

4.2. Electric Tricycle

There are different types of tricycle such as delta type, tadpole type, sidecar tricycle type, but the delta type tricycle is most suitable because of its parameters dynamic stabilities, braking operation, turning operation, acceleration, comfort, visibility angle, height such are better than any other type of tricycle [16]. By Computer Aided Modeling and Finite Element Analysis method, Electric tricycle is made and tested.

4.2.1. Computer Aided Model

CAD model is made with Software named SOLIDWORKS. 2D and 3D models can be made with SOLIDWORKS. Design of component starts with Part design as a first step followed by assembly. The model of component in SOLIDWORKS contents 3D geometries could be made with surfaces, edges, faces [22]. The model of tricycle is made with 3D geometries tools includes beams, weldment joints, surfaces and edges.



Figure 12. Isometric view of Conceptual design of electrical tricycle

CAD model of tricycle made with SOLIDWORKS is shown in the figure 12. Model contains Frame structure, steering, wheel hubs, braking space, wheels, tires motor space, and shock absorbers. Motor, Batteries, Motor controller and other operational wiring parts are not made in CAD model. Some parts simply adopted from old model of electric moped are Motor, Batteries, Motor Controller, Wheels with brakes, steering geometry and shock absorbers for all wheels. The focus of the research methodology is to modify the frame of old electric moped of two-wheeler into frame for three-wheeler vehicle.

Frame of the tricycle is made with hollow pipes connected with welded joints. The front pipe which will provide inside space for steering pipe has to take more load than other thus, the size of the pipe is take bigger than other. Also, the vertical pipes connected to at the rear side of the vehicle which

would have load of rider is also taken bigger than other pipes. All other pipes are smaller in size which would be proven enough strong by further analysis. The design of frame is shown as below figure 13.

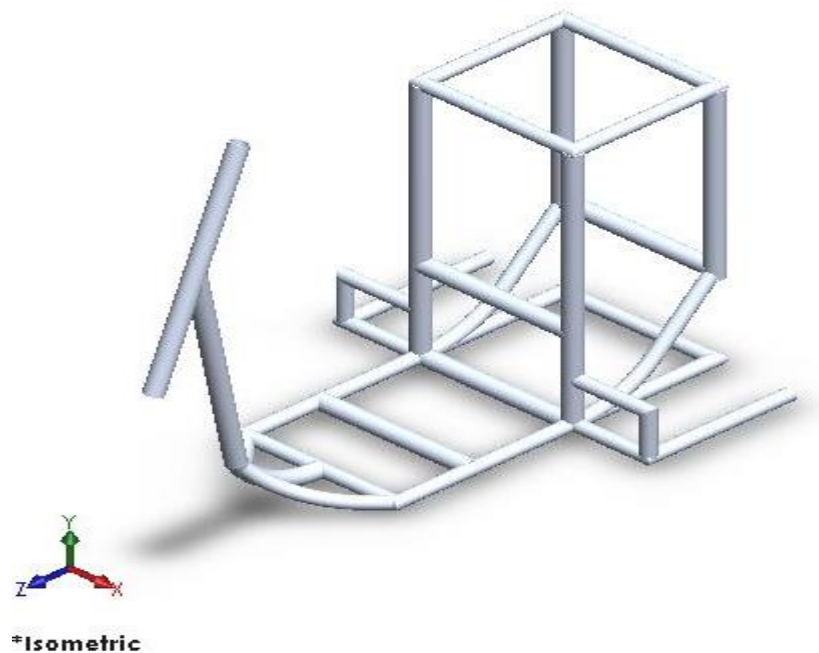


Figure 13. Frame of Tricycle

In the frame geometry there are two types of hollow pipers are used as follows.

1. 26.9X3.2
2. 33.7X4.0

Both types of pipes are standardised by International Organisation for Standardization. In the 1st pipe 26.9 mm is the outer diameter and 3.2 mm is the thickness of the pipe hence 20.5 is the inner diameter of the pipe. This type of pipes has been used for most of the geometry where there is a rider's foot space, as all connecting pipes, connecting pipers as rear side which will be further connect with shock absorber.

The 2nd type of pipe has 33.7 mm outer diameter. 4.00 mm inner diameter thus, it has calculated 25.7 mm inner diameter. This type of pipe has been used in the construction of frame which area has to work with more load compared to other area. Such heavy load carrying area could be area which provides space for steering geometry and the pipes which directly holds the rider's weight. The hollow pipes are connected with welded joints as it is the most suitable joining process for such geometry.

4.3. Material for frame

Aluminium Alloy has been chosen for construction of Frame. Aluminium alloy is most used metal for frame construction like. Other major used material used for component is steel. However, Aluminum Alloy could be cheaper in price, lighter in weight, more reliable in comparison of structural steel [23]. Frame has to withstand loads such as bending load, torsion load, lateral load while braking, remote load while steering operation. The material properties of Aluminum Alloy and Structural Steel is compared below.

Table 3. Properties of Aluminum alloy [24]

Aluminum Alloy		
Property	Value	Unit
Density	2770	Kg*m ⁻³
Coefficient of Thermal Expansion	2.3E-05	C ⁻¹
Young's Modulus	7.1E+10	Pa
Poisson's Ratio	0.33	
Bulk Modulus	6.9608E+10	Pa
Shear Modulus	2.6692E+10	Pa
Tensile Yield Strength	2.8E+08	Pa
Compressive Yield Strength	2.8E+08	Pa
Tensile Ultimate Strength	3.1E+08	Pa

Table 4. Properties of Structural Steel [24]

Structural Steel		
Property	Value	Unit
Density	7850	Kg*m ⁻³
Coefficient of Thermal Expansion	1.2E-05	C ⁻¹
Young's Modulus	2E+11	Pa
Poisson's Ratio	0.3	
Bulk Modulus	1.6667E+11	Pa
Shear Modulus	7.6923E+10	Pa
Tensile Yield Strength	2.5E+08	Pa
Compressive Yield Strength	2.5E+08	Pa
Tensile Ultimate Strength	4.6E+08	Pa

Density of Structural steel is higher than Aluminum Alloy thus, the weight of structural steel is also higher. However, Values of Properties such as Co-efficient of Thermal expansion, Young’s Modulus, Poisson’s ratio, Bulk modulus, shear modulus, tensile yield strength, compressive yield strength and tensile ultimate strength are higher in Aluminium alloy in comparison of structural steel. Thus, Aluminium Alloy is taken as it is the best suitable material for the frame of the electrical tricycle.

4.4. Boundary conditions of CAD model of Frame for FEA methodology

Finite Element Analysis of frame of electrical tricycle is done with ANSYS 18.1 where five analyses are done on the CAD model of frame which is directly imported to ANSYS 18.1 from SOLIDWORKS. All five analyses are named as Bending, Torsion, Lateral, Longitudinal case and natural frequencies. Different analysis performed with different forces and different fixtures.

Table 5. Notations for Forces and Fixture to the model

A	Remote steering force 1	500 N
B	Remote steering force 2	500 N
C	Bending force 1	981 N
D	Bending force 2	294.30 N
E	Lateral force	50 N
F	Torsion force 1	650 N
G	Torsion force 2	650 N
H	Fixed Support	At Front wheel
I	Fixed Support 2	At rear wheel

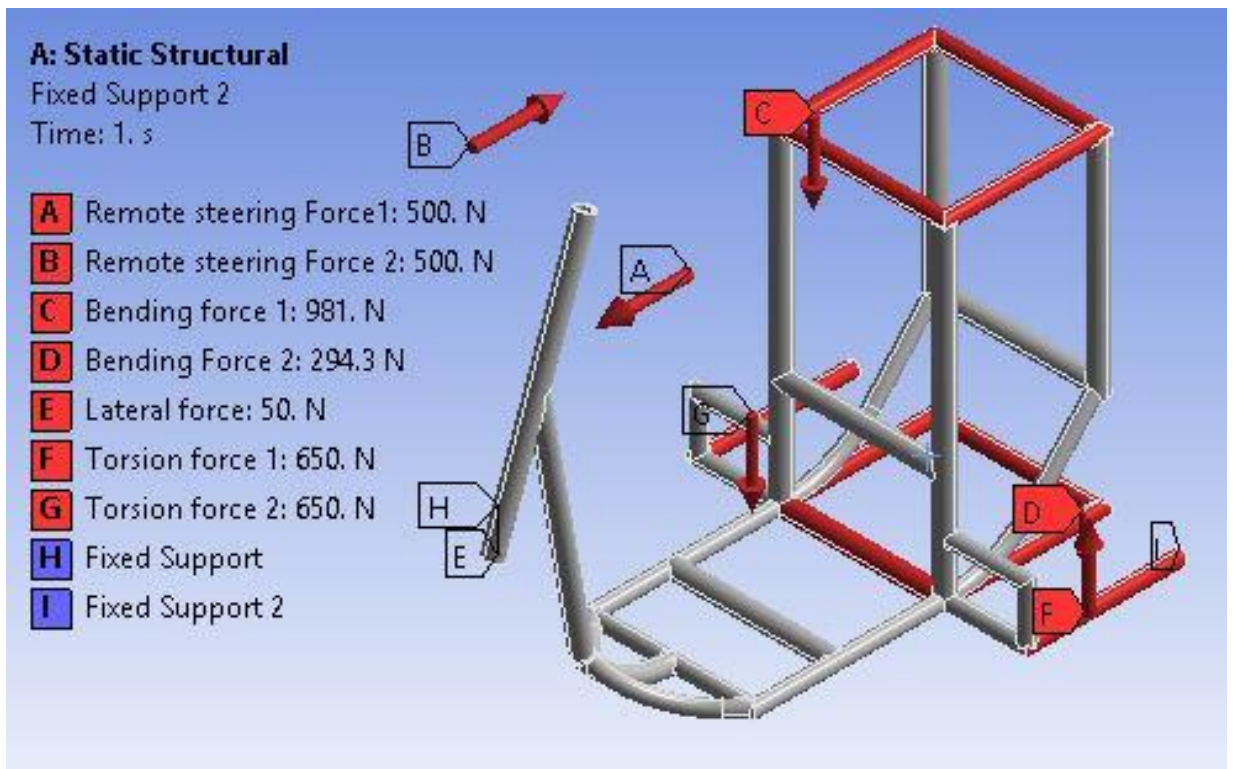


Figure 14. Boundary Conditions

Table 6. Force application of Loading cases

Loading cases	A	B	C	D	E	F	G	H	I
Bending case			✓	✓				✓	✓
Torsion case						✓	✓	✓	
Lateral case					✓				✓
Longitudinal case	✓	✓							✓
Natural frequencies								✓	✓

5. Calculations

Calculations of electric tricycle including dynamic parameters such as speed, aerodynamics, power transmission system and other parts like tires and wheels also the C.G. calculations are proceeded according to the procedure of the book published by “Technologija” by R. Makaras, A. Kersys, M. Felneris, R. Kersys, D. Juodvalkis in 2018 [29].

5.1. Vehicle dimensions

Dimensions of the vehicle is must required for all the calculation of dynamic and kinematic characterise of the vehicles.

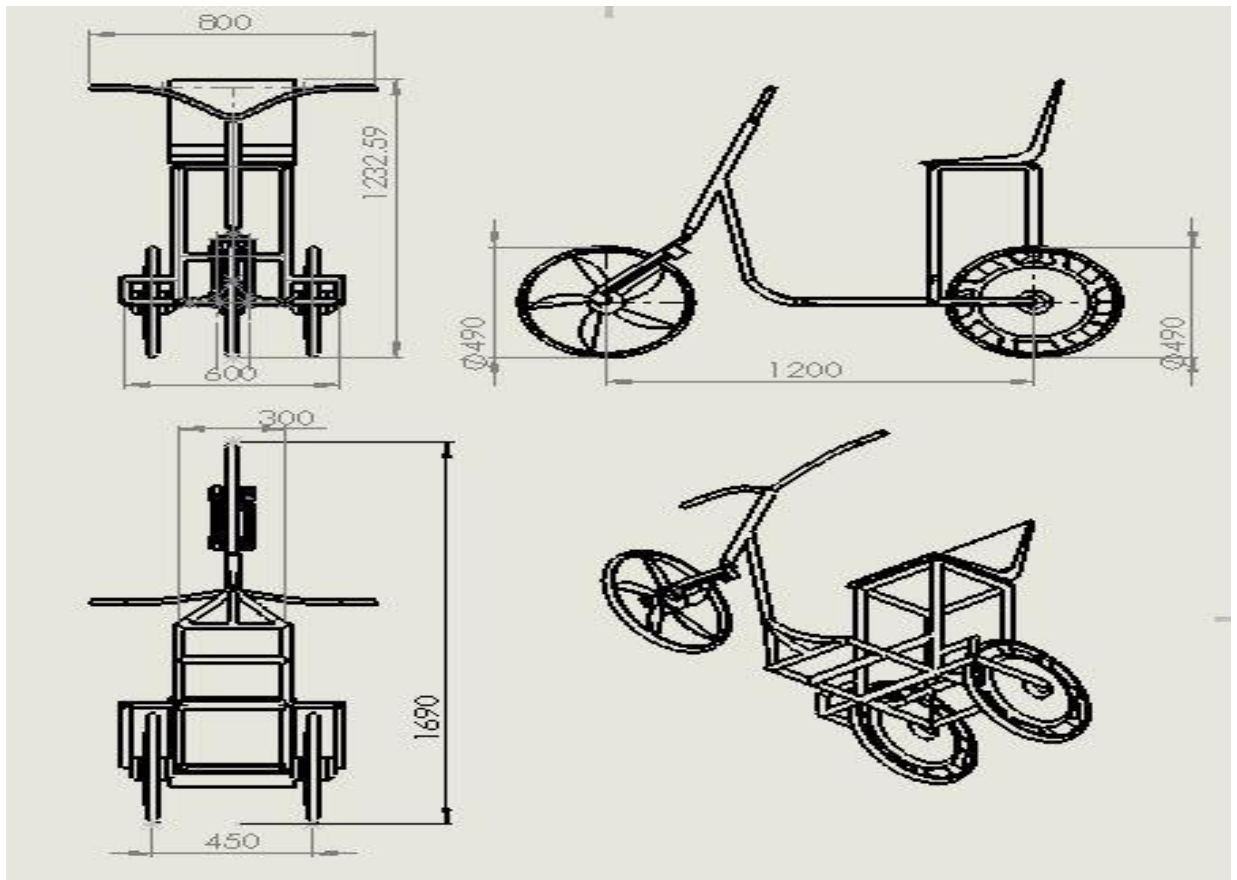


Figure 15. Vehicle Projection and Dimensions

The figure 15 contents four different projections include Front view, Side view, Top view and Isometric view. Vehicle length, vehicle width, vehicle height, wheel base, wheel track and tyre diameter. Isometric view gives better understanding of the 3D geometry.

Table 7. Electric Tricycle Dimensions.

Dimension	Marking	Value	Units
Vehicle Length	La	1690	mm
Vehicle Width	Ba	800	mm

Vehicle Height	Ha	1232.59	mm
Vehicle's wheel base	l	1200	mm
Vehicle Track width in the back	bg	450	mm
Aerodynamic coefficient	Cx	0.7	

5.2. Vehicle technical parameters

Technical parameters of the vehicle such as battery capacity, motor power and torque are predefined characteristics as battery, motor and motor controller are adopted from another electric moped. Chosen electrical vehicle's technical parameters are given in table 8.

Table 8. Technical Parameters

Parameters	Values	Units
No. of driving motors	2	
Arrangement of motors	1-Rear left 2- Rear right	
Motor Power	250	Watt
Motor RPM	500	
Battery Capacity	48v-33ah	Volt-Ampere
Charging time	6-8h	Hours
Travelling Range	65-70 /130	Km/kg
Max. Speed	45	Km/h
Torque	45	Nm

5.3. Vehicle drive scheme, gearbox gear ratios, final drive gear ratio

Considering the operating conditions of comfort, dynamic requirements of the selected vehicle setup, they have transferred units.

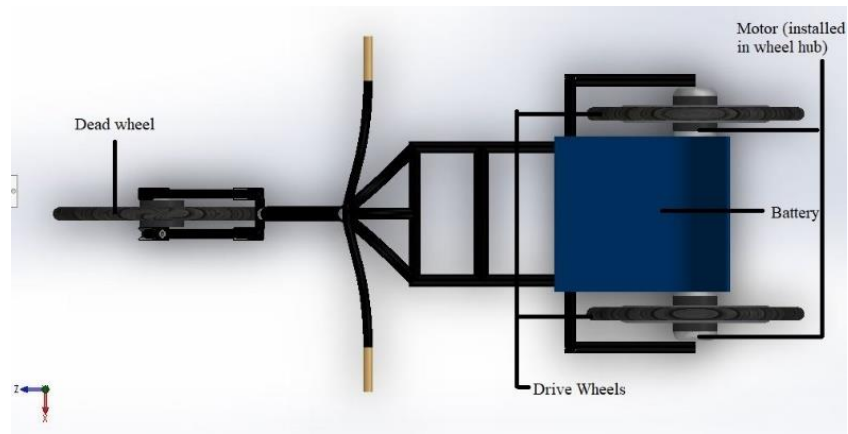


Figure 16. the arrangement of tricycle layout, i.e. rear wheel drive.

Figure 16 Shows that tricycle has front dead wheel which is used to steer the vehicle and both rear wheels are drive wheels. Motors are directly installed in the wheel hub of drive wheels so that there is not additional gear box is required. The motor rpm directly adopted by the wheel so motor it selves acts as a final drive in the vehicle.

Table 9. Gear ratio

Gear ratio	
1 st gear	1:1
Final Gear	1:1
Reverse Gear	N/A

5.4. Vehicle tire dimensions

Every vehicle has different types of tyres for suitable driving conditions and structural conditions. Tyre could be chosen according to characteristics and parameters of tyres. Parameters and characteristics are shown in figure 17:

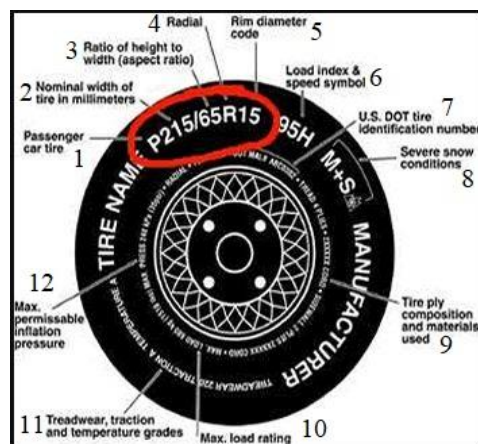


Figure 17. Tyre parameters [25]

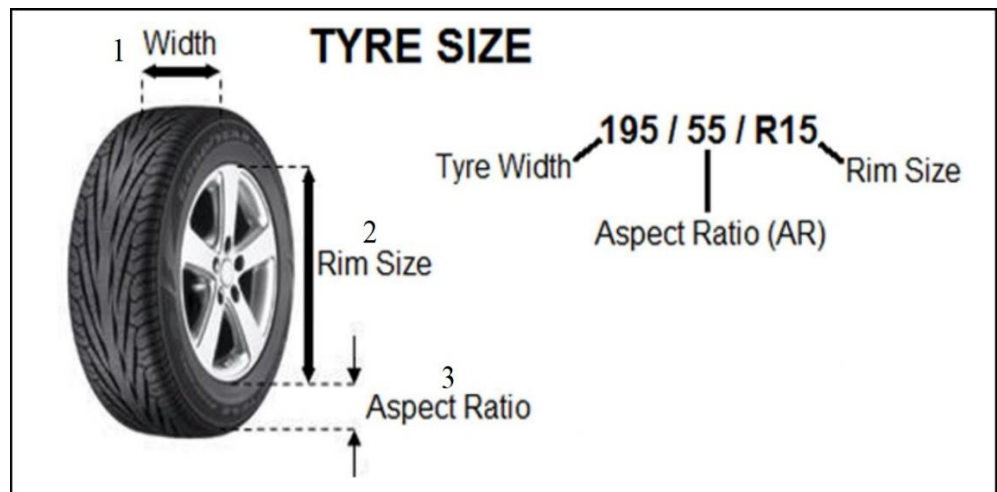


Figure 18. Tyre parameters [25]

The parameters named and cited in the figure 18 are

1. Passenger car tyre
2. Nominal width of tyre in millimetre
3. Ratio of height to width
4. Radial
5. Rim Diameter code
6. Load index and speed symbol
7. U.S. DOT tyre is the Identification number
8. Sever snow condition
9. Tyre ply composition and material used
10. Max. Load rating
11. Treadwear, traction and temperature grades
12. Max. permissible inflation pressure

The parameters cited in the figure 5.4.2 are

1. Width of tyre
2. Aspect ratio
3. Rim size

Index	Max Speed	Index	Max Speed	Index	Max Speed
A1	5 Km/h	D	65 Km/h	Q	160 Km/h
A2	10 Km/h	E	70 Km/h	R	170 Km/h
A3	15 Km/h	F	80 Km/h	S	180 Km/h
A4	20 Km/h	G	90 Km/h	T	190 Km/h
A5	25 Km/h	J	100 Km/h	H	210 Km/h
A6	30 Km/h	K	110 Km/h	V	240 Km/h
A7	35 Km/h	L	120 Km/h	W	270 Km/h
A8	40 Km/h	M	130 Km/h	Y	300 Km/h
B	50 Km/h	N	140 Km/h	Z	240+ Km/h
C	60 Km/h	P	150 Km/h		

Figure 19. Tire speed index Numbers shows what maximum speed is allowed

The tyre used in particular model of tricycle is having dimensions of 90/100 R10. The parameters are shown in table 10 for further calculations.

Table 10. Tyre parameters

Dimension	Marking	Value	mm
Tire width	B	90	mm
Tire height	H	$(B*100)/100=90$	mm
Wheel diameter	d	$10*25.4=254$	mm

5.5. Vehicle dynamic characteristics: maximum speed, acceleration

In table 11 is shown maximum design speed and acceleration parameters:

Table 11. table Vehicle dynamic parameters

Characteristic	Value	Units
Max. designed speed	45	Km/h
Time for 0 to max. speed	10	Sec
Acceleration for max. speed	4.5	m/s^2

Vehicle weight distribution of the front and rear axles, calculations of the vehicle center of gravity using program "MAS1"

5.5.1. The main vehicle's components arrangement in scheme (on lateral projection);

For calculations of vehicle mass distribution for the vehicle components and vehicle center of gravity. Vehicle is divided into separate parts. Components which have significant influence for vehicle mass must be selected as separate component. For further calculations must be accepted that a one person is driving the tricycle (weight is 100kg). The main vehicle components to scale are shown on Figure 20 using coordinate axis Y, Z on lateral projection.

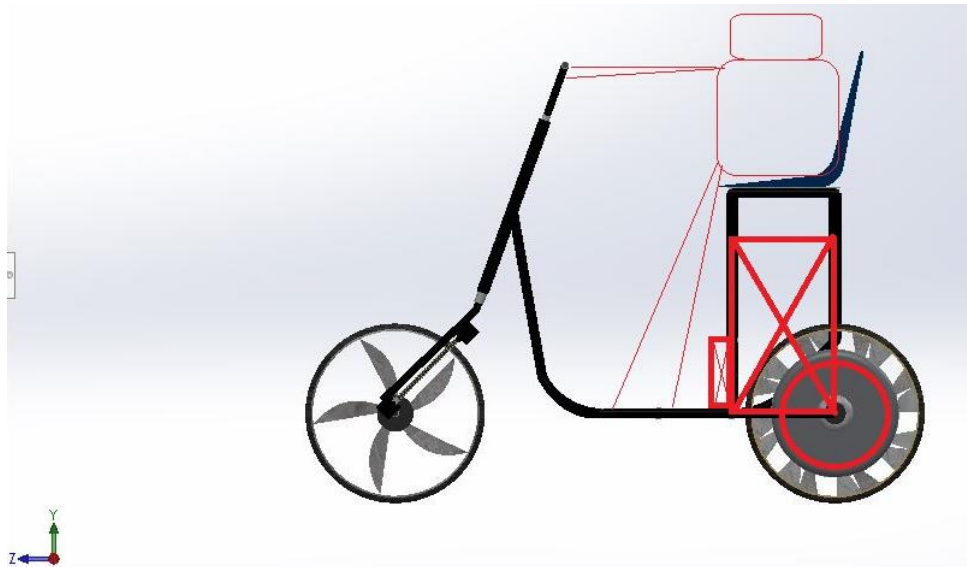


Figure 20. Vehicle Component and user location layout

5.6.2 The main vehicle's components arrangement on coordinate axis x and z (data will be used for further calculations with "MAS1")

Calculation is done with max. components of the vehicle. Approximate values have been taken for the component whose exact values are unknown. Some components are combined for example wheel could be combination of wheel rim, tyre and brake system for particulate. Components are shown in table 12.

Table 12. Vehicle Elements with weight distribution and location

No.	Elements	Weight (kg)	X axis (mm)	Y axis (mm)	Z axis (mm)
1.	Battery	30	0	520	1350
2.	Motor R.H. side	10	285	300	1445
3.	Motor L.H. side	10	-285	300	1445
4.	Motor controller	1	0	300	1160
5.	Front L.H. Shock absorber	2	-45	400	470
6.	Front R.H. Shock absorber	2	45	400	470
7.	Rear L.H. Shock absorber	2	-150	500	1445
8.	Rear R.H. Shock absorber	2	150	500	1445
9.	Front wheel	1.5	0	245	245
10.	Steering system	3	0	600	500
11.	Rear left wheel	1.5	-225	245	1445
12.	Rear right wheel	1.5	225	245	1445

13.	Chassis	30	0	300	700
-----	---------	----	---	-----	-----

5.5.2. Vehicle element distance from the starting of the front tyre on coordinate system.

	Name	weight, kg	Y, coordinate, mm	Z, coordinate, mm
18	Components			
19	Battery	30	520	1350
20	Motor R.H. side	10	300	1445
21	Motor L.H. side	10	300	1445
22	Motor controller	1	300	1160
23	Front L.H. Shock absorber	2	400	470
24	Front R.H. Shock absorber	2	400	470
25	Rear L.H. Shock absorber	2	500	1445
26	Rear R.H. Shock absorber	2	500	1445
27	Front	1.5	245	245
28	Steering system	3	600	500
29	Rear left wheel	1.5	245	1445
30	Rear right wheel	1.5	245	1445
31	Chassis	30	300	700
32				

Figure 21. Data for C.G. Calculation

Vehicle weight distribution on the center of gravity			
Base, mm	Weight kg	Results	
1200	96.5	Weight, kg	96.5
		Yc, mm	387.6
		Zc, mm	1092.5

Figure 22. Result of Calculated C.G.

5.5.3. Comparison of calculated Centre of Gravity with SOLIDWORKS model

Override center of mass:

X: Y: Z:

As defined in:

Figure 23. Calculated C.G. in SOLIDWORKS

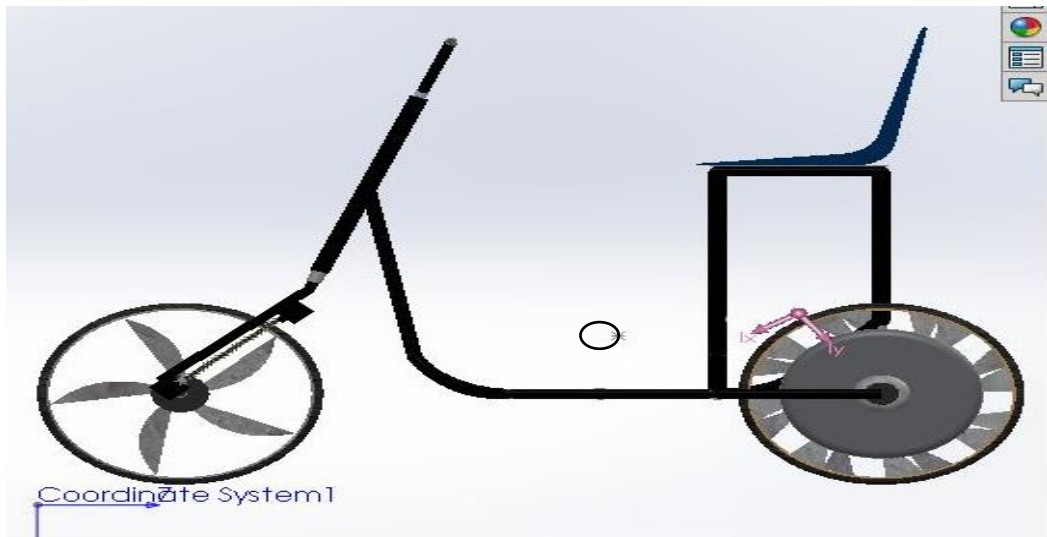


Figure 24. Comparison of C.G. calculated in SOLIDWORKS and by manual

The Manual calculated Centre of gravity of the vehicle is coordinates as $x=0$, $y=387.6$ and $z=1.92.5$. This manual calculate C.G. is shown in the figure as a gray “ * ”. Where C.G. calculated by SOLIDWORKS solver is shown with pink coloured aero. While comparing both the result the difference is 129.1 mm in Y axis and 210.58 mm in Z axis.

The reason of this difference in between both the result is because of the mass properties of the parts and the centre points of the elements. In the manual calculation mass properties are more precise compare to SOLIDWORKS model as software model is having just a mass of material properties but not the actual mass of all parts like motor and battery.

However, software model is more accurate in Centre points of the parts compare to manual calculations as it is purely assumed according to the dimensions of the vehicle. Thus, both results are having difference of almost 10 cm in Y axis and Z axis.

5.6. Theoretical calculations of vehicle gearbox

Wheel static radius calculation

Pneumatic wheel because of its elasticity and due to the changes of centrifugal forces, does not remain constant, radius is changing. Designated following wheels rolling radius:

- 1) Free r_0 (Figure 5.7.1) or maximum stationary and an unloaded wheel radius, it depends only on pressure in tire.
- 2) Static r_{st} (Figure 5.7.1) – minimum distance from the wheel loaded by the vertical force axis to the ground. This radius depends on the pressure in the tire, vertical load and type of the tire.

3) Wheel rolling radius (kinematic) – rolling wheel loaded with vertical force and tractive force radius.

4) Wheel dynamic radius – tractive forces loading the wheel, compresses tread elements which are in contact, therefore road travelled per one-wheel revolution will be less than wheel circumferential length.

Free wheel radius r_0 , is found from expression 5.6.1

$$r_0 = 0.5d + 0.001B + H(\text{mm}); \quad \text{expression 5.6.1}$$

$$= (0.5 * 254) + (0.001 * 90) + 90$$

$$= 217.09 \text{ mm}$$

$$r_0 = 217.09$$

Here,

(from table 5.4)

$$d = \text{rim diameter} = 10 \text{ inch} = 254 \text{ mm}$$

$$B = \text{tyre width} = 90 \text{ mm}$$

$$H = \text{tyre height} = 90 \text{ mm}$$

Static wheel radius r_{st} , is found from expression 5.6.2

$$r_{st} = 0.5 * d + \Delta \lambda_s * B \quad \text{expression 5.6.2}$$

$$= (0.5 * 254) + (0.9 * 0.8 * 90)$$

$$= 179.1 \text{ mm}$$

$$r_{st} = 179.1 \text{ mm}$$

here,

$$\Delta \text{ relative tyre height in section} = 90$$

$$\lambda_s \text{ is tyre seat (0.8 to 0.95);}$$

Tyre seat coefficient depends on type of the tire. Low profile tires or high-pressure tires “seat” coefficient is bigger than high profile tires or low-pressure tires “seat” coefficient.

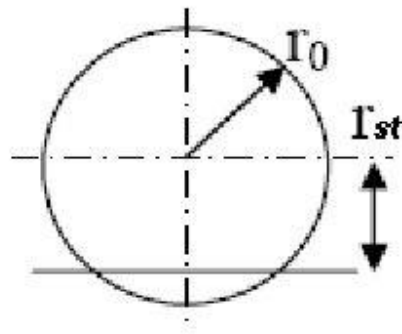


Figure 25. Wheel rays

In calculations of wheel static radius, wheel seat is evaluated due to the load forces.

Low pressure tires $\lambda_s=0,93$

High pressure tires $\lambda_s=0,95$,

Light car's diagonal tire $\lambda_s=0,85.....0,9$

Light car's radial tire $\lambda_s=0,8.....0,85$

5.6.1. Theoretical gearbox transmission ratio calculations

Final drive generally is called couple of bevel gears, which is on the transaxle's reducer in four-wheeler cars but here, motor is directly connected with the wheel hub as shown in Figure 5.7.2. Theoretical transmission ratio of final gear - U_{pp} (expression 3.4) can be found, when direct gear is actuated (gear which has gear ratio of 1 or close to that number).



Figure 26. Basic construction of motor to wheel as powertrain [26]

$$U_{pp} = \frac{0.105 * r_{st} * n N}{v_{max}}; \quad \text{expression 5.6.3}$$

$$U_{pp} = \frac{0.105 * 179.1 * 500}{45}$$

$$U_{pp} = 208.83$$

Here:

nN – motor revolutions at maximum power (rpm);

v_{max} – vehicle maximum speed (m/s);

r_{st} – wheel static radius (m);

Checking Anti-slip conditions Created moment force to the drive wheel of the vehicle's power supply component and transmission is $-P_b$

$$P_b = M_{max} * U_{tr} * U_1 * \eta_{tr} * \frac{Kk}{r_{st}}$$

Here:

η_{tr} = Transmission efficiency coefficient (0.88/0.98) = 0.92

For the drive wheels anti-slip conditions longitudinal traction force at the periphery of the wheel is required.

$$P_{bsk} = \frac{G * l * \varphi_x * \cos \alpha}{l - hc * (\varphi_x + f_a)}$$

Here:

G – vertical gravity of the vehicle weight for the driving axles (N) (Values from „MAS1“);

l – vehicle base (m);

φ_x – grip factors (0,75 ÷ 0,85);

$\alpha = 0^\circ$ - slope (uphill) factor;

hc – the vehicle's center of gravity height (m) („MAS1“).

f_a – resistance coefficient (0,01);

Anti-slip condition is true if – $P_{bsk} \geq P_b$;

However, in the case of the electrical vehicle having motor directly fitted in the wheel hub the calculation of gear ratio is not required. In terms of gear ratio here chances of power loss due to different gear ratio and slipping of gears are zero.

5.7. The dynamics of the wheel

5.7.1. Wheel angular velocity

$$\omega_{ri} = \frac{0.105 * n_i}{U_{pp}}$$

Here,

ω_{ri} – wheel angular velocity at i – th engine speed. Engine speed range from idle speed till maximum speed is divided into 8 intervals (example: if engine idle speed has 1000 rpm, and maximum speed has 8000 rpm, then intervals are divided at every 1000 rpm). Table is made named 13.

Table 13. Angular Velocity

No.	N_i (RPM)	ω_{ri} (rad/s)
1.	5.625	0.0028
2.	11.25	0.005
3.	16.875	0.008
4.	22.5	0.011
5.	28.125	0.014
6.	33.75	0.016
7.	39.375	0.019
8.	45	0.022

5.7.2. Wheel moment

$$M_{ri} = (M_{max} * U_{pp} * \eta_{tr}) - (J_r * U_{pp}^2 * \eta_{tr} * \omega_{ri})$$

$$M_{ri} = (45 * 208.83 * 0.92) - (0.038 * 208.82 * 0.92 * \omega_{ri})$$

Here,

M_{max} - Maximum torque (Nm);

$J_r = 0.038 \text{ (kgm}^2\text{)}$ – wheel moment of inertia;

ω_{ri} – i th wheel angular velocity (rad/s) (values from table 14);

Table is created;

Table 14. Wheel moment

No.	ω_{ri} (rad/s)	M _{ri} (Nm)
1.	0.0028	8.64553
2.	0.005	8.64552
3.	0.008	8.64550
4.	0.011	8.64547
5.	0.014	8.64545
6.	0.016	8.64544
7.	0.019	8.64542
8.	0.022	8.64539

Graph must be created $M_{ri} = f(\omega_{ri})$;

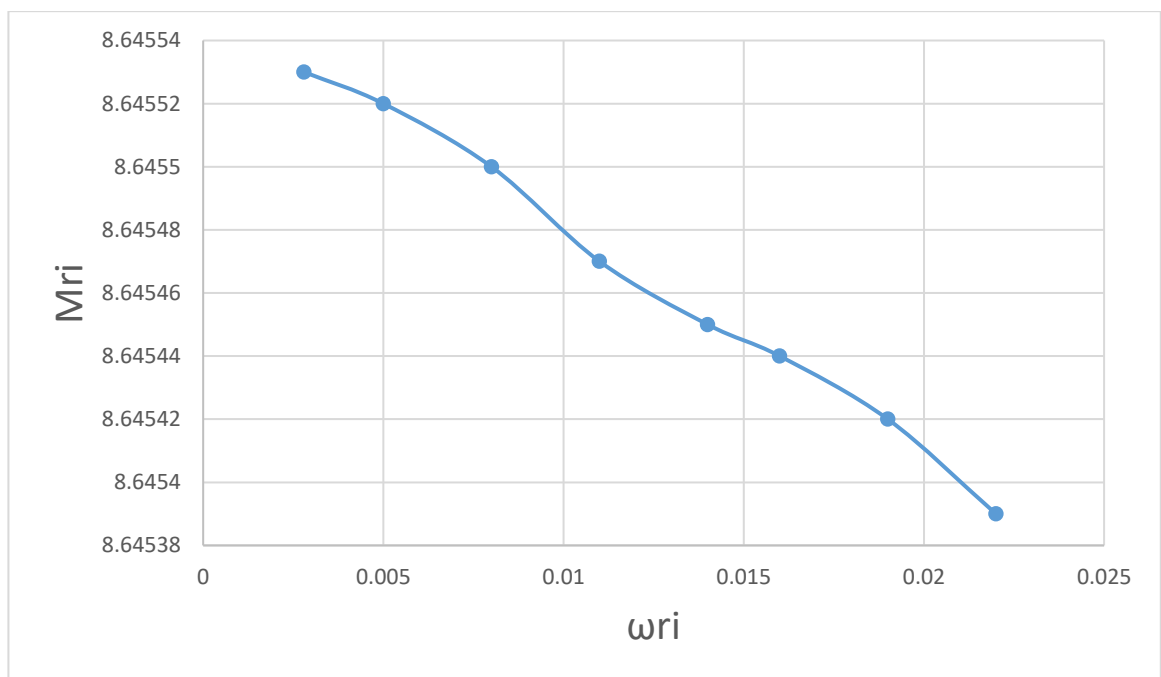


Figure 27. Graph of wheel moment to wheel angular velocity

Wheel angular velocity and Wheel moment both can be represented in respect to time. So, while comparing both the case it is obtained that the time interval remains same thus neglected from the result. For the time interval by applying of power angular velocity and wheel moment will have significant changes in the values.

The relation in between the both is shown in the graph that on the angular velocity of 0.0028 rad/s wheel moment will be 8.64553 Nm which will gradually decreases with increasing the angular

velocity so it to be said that wheel moment relatively increases with angular velocity decreases and vice versa.

5.7.3. Dynamic radius of the wheel

$$r_d = r_{st} - \lambda * M_{r \max}$$

$$\lambda = 1000 * (H/B) * (P/G)$$

$$\lambda = 1000 * (90/90) * (0.20/96.5) = 2.07$$

$$r_d = 179.1 - 2.07 * 45 = 85.95 \text{ mm.}$$

Here,

P- pressure in the tires (MPa) = 0.20 Mpa

$M_{r \max}$ - maximum torque of the wheel (Nm)=45;

4.4 Kinematic radius of the wheel

$$R_{kim} = (V_{\max} / \omega_{\max})$$

$$= (12.5 / 0.022)$$

$$= 568.18 \text{ mm}$$

Here,

V_{\max} -vhicle max. speed

$$= 45 \text{ km/h}$$

$$= 12.5 \text{ m/s}$$

ω_{\max} – max. angular velocity (rad/s) = 0.022

5.8. Forces acting on the vehicle;

5.8.1. The motor torque reserve

The motor nominal torque - M_n ;

$$M_n = \frac{9549 * N_{\max}}{nN};$$

$$= \frac{9549 * 1.1}{500}$$

$$M_n = 21.00 \text{ Nm}$$

Here:

N_{max} – maximum power of the motor (kW);

n_N – motor rpm on maximum power;

The motor torque reserve - kMa ;

$$kMa = \left(\frac{M_{max} - M_n}{M_{max}} \right) * 100\%$$

$$= \left(\frac{45 - 21}{45} \right) * 100\%$$

$$kMa = 0.533 \text{ Nm}$$

Where,

M_{max} – maximum torque of the motor (Nm).

5.8.2. The power loss in the vehicle

Mechanical losses in the transmission depends on the adhesion of the teeth, tightening size of the bearing, front-wheel geometry, the size of the air pressure in the tires, brakes and clutch mechanisms adjustment quality and condition, as well as transmission oil hydraulic resistance. Friction forces in transmission are higher, if transmission nodes were manufactured with low precisions.

The power loss in transmission - N_{tr} ;

$$N_{tr} = 10^{-3} * (P_{tr0} * V_i + k_{tr} * v_i^2);$$

Here,

$P_{tr0} = 13 \text{ (N)}$ – constant resistance force in the transmission;

$k_{tr} = 3.5 \text{ (Ns/m)}$ – transmission damping constant;

v_i – vehicle kinematic speed at i – th rpm

$$v_i = \frac{0.105 * n_i * r_k}{U_{pp}}$$

$$= \frac{0.105 * n_i * 45}{208.83}$$

In the case of electrical tricycle with motor located in wheel hub directly, no gear mechanism attached as mentioned before also clutch and flywheel mechanism is also eliminated as power is directly generated by the motor but not with engine thus there would be zero power loss by gear teeth. The power loss could be resultant because of braking application, traction, tyre resistance also by tyre air pressure.

Table 15. Vehicle kinematic speed and transmission power loss calculation

ni (rpm)	Vi(m/s)	Ntr(kw)
62.5	1.4141	0.025
125	2.75	0.062
187.5	4.125	0.11
250	5.5	0.17
312.5	6.875	0.24
375	8.25	0.34
437.5	9.625	0.44
500	11	0.56

Transmission power loss dependence on the vehicle's kinematic speed. The relation of transmission power to kinamatic speed is shown in figure 28.

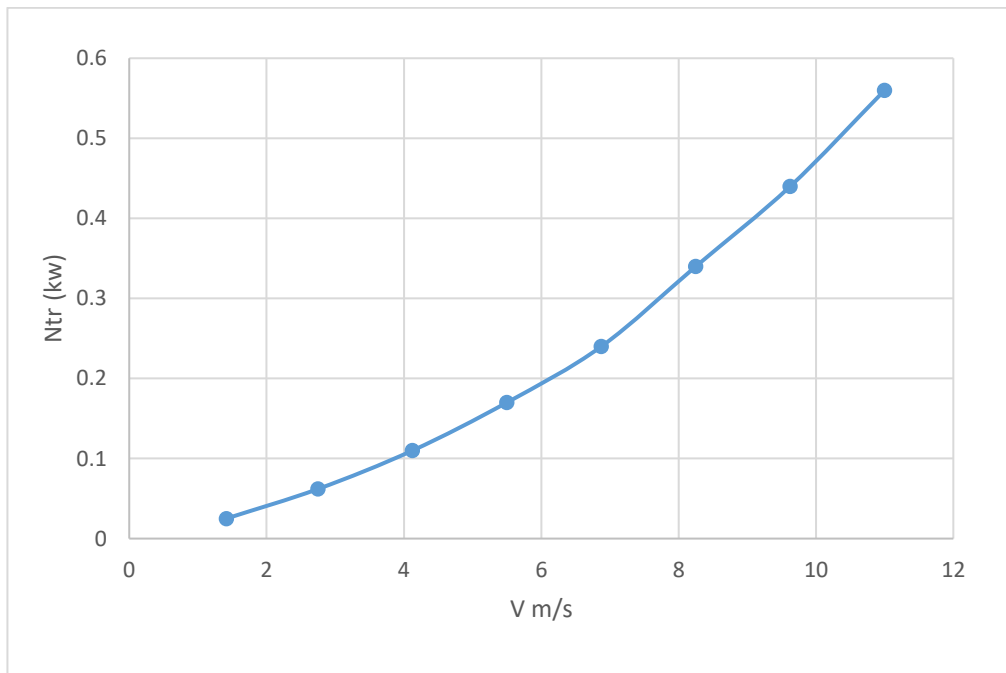


Figure 28. Vehicle kinematic speed to transmission power loss

Here, X axis shows the values of vehicle kinematic speed where Y axis determines the values of transmission power loss. Here, the transmission power loss is relatively increases with vehicle kinematic speed. When vehicle kinematic speed is 1.41m/s the transmission power loss is 0.025 kw. Which reaches to the 0.56 kw max when the kinematic speed is max. off 11 m/s. So, the power loss is higher with higher speed and its less in lower speed.

5.9. Wheel rolling resistance force

$$P_r = \frac{G}{n} * f_a * \cos\alpha;$$

Here,

G – vehicle weight force (N)

G=m*a; (a= 4.5 m/s² from tabl 1.5)

n – number of the wheels;

f_a – wheel rolling resistance force (when vehicle rolls on asphalt or cement concrete (0,007 – 0,015)).

α – gradient, is assumed that the angle is equal 0.

$$G = 96.5 * 4.5 = 434.25 \text{ N}$$

$$P_r = \frac{434.26}{2} * 0.015 * \cos 0;$$

$$P_r = 3.2569 \text{ N}$$

5.10. Air resistance force

Vehicle's model (cross-sectional) area;

$$F_M = 0.778 (B_a H_a)$$

B_a- vehicle width;

H_a- vehicle height.

Approximately F values:

- Large bus – 4...6.5 m²;

- Truck – 2...5 m²;

- Light car – 1.5...2.8 m²;

- Race car – 0.75...1.5 m².

Air resistance force

$$P_{oro} = 0.61 * C_x * F_M * v_i^2;$$

Here,

C_x – vehicle’s aerodynamic drag coefficient. Usually can be found on vehicle’s technical characteristics. If there is no information, table below can be used.

Body as a cube has $C_x = 1$,

Sphere (ball) $C_x = 0.25$,

Falling water drop $C_x = 0.013$,

Light car $C_x = 0.1...0.7$.







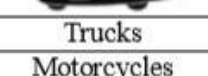
Body type	C_x	Power (kW), which is required to overcome air resistance at different speed. Middel area is assumed $F = 2 \text{ m}^2$			
		40 km/h	80 km/h	120 km/h	160 km/h
	0,5...0,7	1	7,9	27	63
	0,5...0,6	0,91	7,2	24	58
	0,4...0,55	0,78	6,3	21	50
	0,3...0,4	0,58	4,6	16	37
	0,2...0,25	0,37	3	10	24
	0,23	0,38	3	10	24
	0,15...0,20	0,29	2,3	7,8	18
Trucks	0,8...1,5	-	-	-	-
Motorcycles	0,6...0,7	-	-	-	-
Buses	0,6...0,7	-	-	-	-
Smooth buses	0,3...0,4	-	-	-	-

Figure 29. Various drag co-efficient data according to vehicle categories [27]

Frontal area of vehicle F_M : 0.43658817

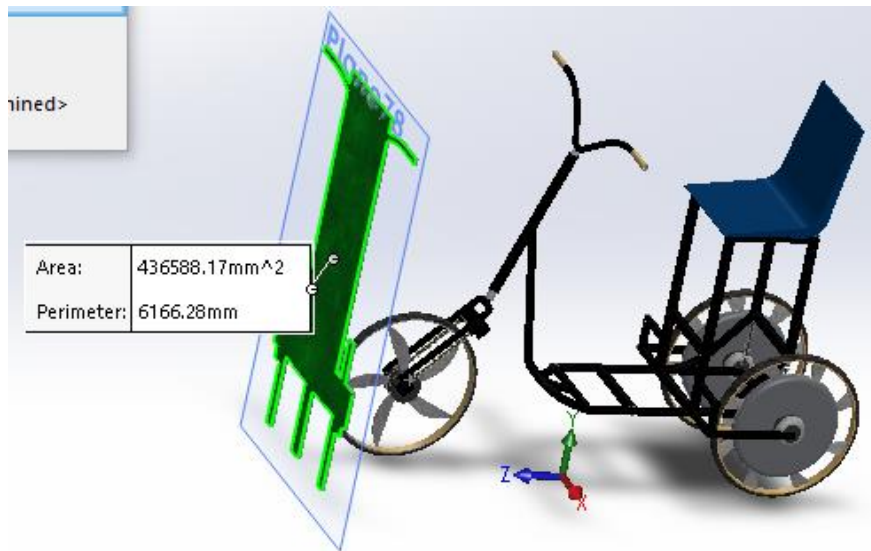


Figure 30. Frontal cross-sectional area of vehicle

Table created for different air resistance force on different speed:

Speed is divided from 0 to max in equal range.

Table 16. Vehicle speed and Air resistance data

Vi (m/s)	Poro (N)
0.8333	0.1294
1.6666	0.5177
2.5000	1.165
3.3333	2.0706
4.1666	3.2360
5.0000	4.66
5.8333	6.3355
6.6666	8.2678
7.5	10.485
8.3333	12.9434
9.1666	15.6625
10	18.64
10.8333	21.8747
11.6667	25.3712
12.5	29.125

Airforce affection on the vehicle running condition in different speed is calculated and mentioned as table 16.

Dependence on air resistance force and vehicle speed is created.

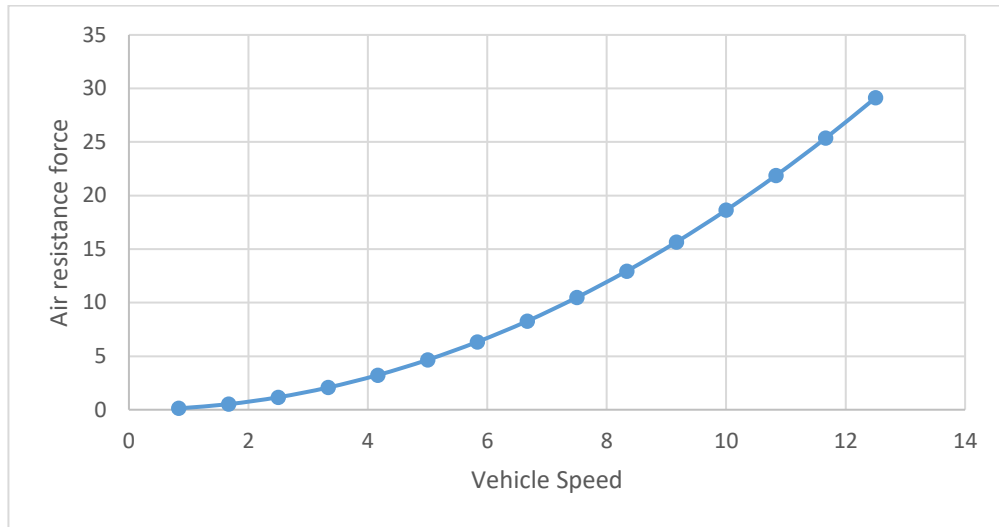


Figure 31. Air resistance with reference to vehicle speed

In figure 31 vehicle speed dependence on the air resistance force acting on the vehicle in running condition is shown. The vehicle speed is given in m/s. The air resistance force is given in N. The air resistance force acting on the vehicle is co relates with speed. It continuously increases with increasing speed and it decreases with deceleration. So, Air resistance force will be 0.1294 N in the starting speed of 0.8333 m/s. The air resistance force increases and reaches to the 29.125 N on the top speed of the vehicle which is 12.5 m/s.

5.11. Vehicle pull (traction) analysis

Vehicle pull analysis shows vehicle dynamic capabilities depend on gear, vehicle speed and engine operating condition. Natural vehicle transmission ratio i – th;

$$U_{ntr}(i) = U_{pp} * U_i$$

Here,

U_{pp} – Final drive ratio- 208.83

U_i – ith gear ratio but the vehicle has no gear mechanisms. Motor directly connected to the wheel hub. So, U_i is considered 1 here.

$$U_{ntr}(i) = 208.83 * 1$$

$$U_{ntr}(i)=208.83$$

Kinematic vehicle speed, when i – th gear is on and i – th rpm n_i ;

$$V_{ki} = \frac{0.105 * n_i * r_k}{U_{ntr}}$$

$$V_{ki} = \frac{0.105 * n_i * 568.18}{208.83}$$

Vehicle pull force;

$$P_t(i) = \frac{M_v(i) * U_{ntr}(i) * n_{tr}}{r_d}$$

Here: $M_v(i)$ – motor torque at i – th rpm. Rpm range must be divided at least in 6 parts, from free (idle) to maximum rpm.

η_{tr} – transmission efficiency.

Air resistance force;

$$P_{oro} = 0.61 * C_x * F_M * v_i^2;$$

Vehicle movement inertia force;

$$P_{in}(i) = P_t(i) - P_{oro}(i).$$

Table 17. Data calculation for 8 interval of RPM for $V_k(i)$, $P_t(i)$, $P_{oro}(i)$, $P_{in}(i)$

$n_i(\text{rpm})$	$M_v(i)$ (Nm)	Gear in use	U_{tr}	$V_k(i)$ (m/s)	$P_t(i)$ (N)	$P_{oro}(i)$	$P_{in}(i)$
62.5	15	1	208.83	1.785	33.45	0.58	32.87
125	23			3.5	51.29	2.27	49.02
187.5	37			5.25	82.51	5.12	77.39
250	45			7.0	100.35	9.114	91.24
312.5	40			8.7	89.2	14.04	75.16
375	32			10.5	71.36	20.50	50.86
437.5	27			11.256	60.21	23.54	36.67
500	21			12.50	46.83	29.06	17.76

Vehicle pull force - $P_t(i)$ dependence on vehicle kinematic speed - $v_k(i)$ is drawn in figure 6.

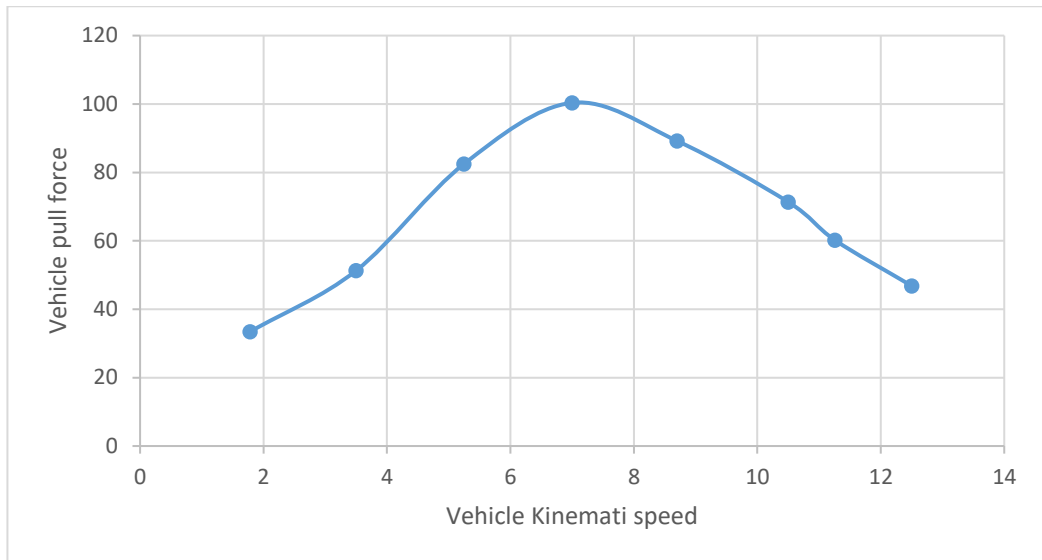


Figure 32. dependence of vehicle kinematic speed on Vehicle pull force

Vehicle pull force which resist the vehicle to the opposite direction of moving is depends on the vehicle kinematic speed. When the kinematic speed increases the vehicle pull force also increases. But this dependence reaction happens with particular speed only after that the vehicle pull force will decrease on certain level as shown in figure the line goes upward and come back to downwards again. Here, the vehicle pull force is minimum in starting is 33.45 N on the kinematic speed of 1.78 m/s reaches to its max which is 100.35 N on the kinematic speed of vehicle on 7.0 m/s. On the continue cycle hen speed raised and reaches to its max. on 12.5 m/s the vehicle pull force will decreases on certain level to 46.83 N.

5.12. Vehicle movement in the corner

Vehicle controllability

Turning radius of the vehicle is to be calculated. For that require data are wheel base and steering angle.

W - Wheel base = 1200mm

α - Steering turning angle = 15°

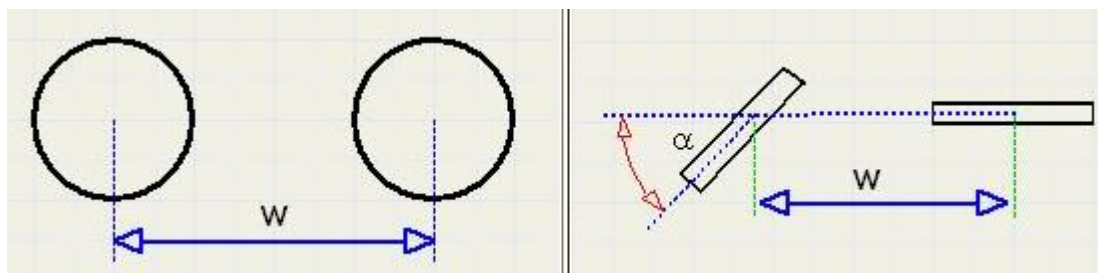


Figure 33. Wheel base and steering turning angle α

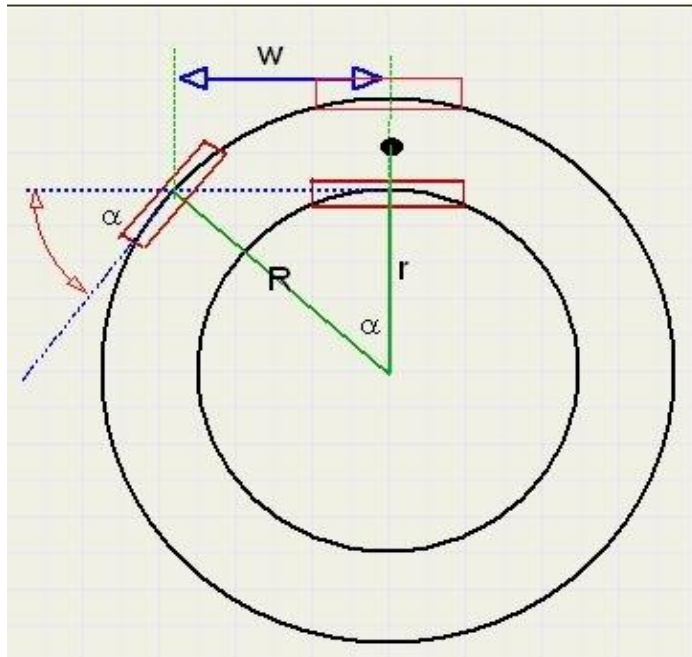


Figure 34. Turning radius

In tricycle and bicycles front wheel and rear wheels turning circles have same centre point and the radius and direction will be perpendicular as shown in figure 34.

Turning radius of front wheel is taken as R and turning radius of rear wheel is taken as r.

$$\sin\alpha = \frac{W}{R};$$

$$\therefore R = \frac{W}{\sin\alpha} = \frac{1200}{\sin 15} = 4636.44 \text{ mm} = 4.63 \text{ m}$$

Also,

$$\tan\alpha = \frac{W}{r}$$

$$\therefore r = \frac{W}{\tan\alpha} = \frac{1200}{\tan 15} = 4478.46 \text{ mm} = 4.47 \text{ m}$$

$$\text{Vehicle turning radius } V_{tr} = \frac{R+r}{2} = 4.55 \text{ m}$$

Vehicle turning radius varies with different turning angle, thus 4 different steering angles are taken for various turning radius.

Table 18. Turning radius for different steering angles

α	R
15	4.63
20	3.50
25	2.83
30	2.40

Here, it is to be said that turning radius of vehicle decreases with increasing of steering angle.

Vehicle centrifugal force acting in the corner;

$$P_{is} = m_a \frac{v(i)^2}{R_i};$$

Here:

m_a – vehicle mass;

$v(i)$ – vehicle movement speed (m/s);

R – corner radius (m).

$$P_{is} = 96.5 \frac{v(i)^2}{R_i}$$

Table 19. Pis calculated for four different values

V(i) (m/s)	Pis (N)			
	R=25 (m)	R=50(m)	R=75(m)	R=100(m)
7.5	217.125	108.56	72.37	54.28
8.5	278.88	139.44	92.96	69.72
9.5	348.36	174.18	116.12	87.09
10.5	425.56	212.78	141.85	106.39
11.5	510.48	255.24	170.16	127.62
12.5	603.12	301.56	201.04	150.78

Dependence graph is to be made for vehicle centrifugal force acting at cornering with vehicle speed at different turning radius.

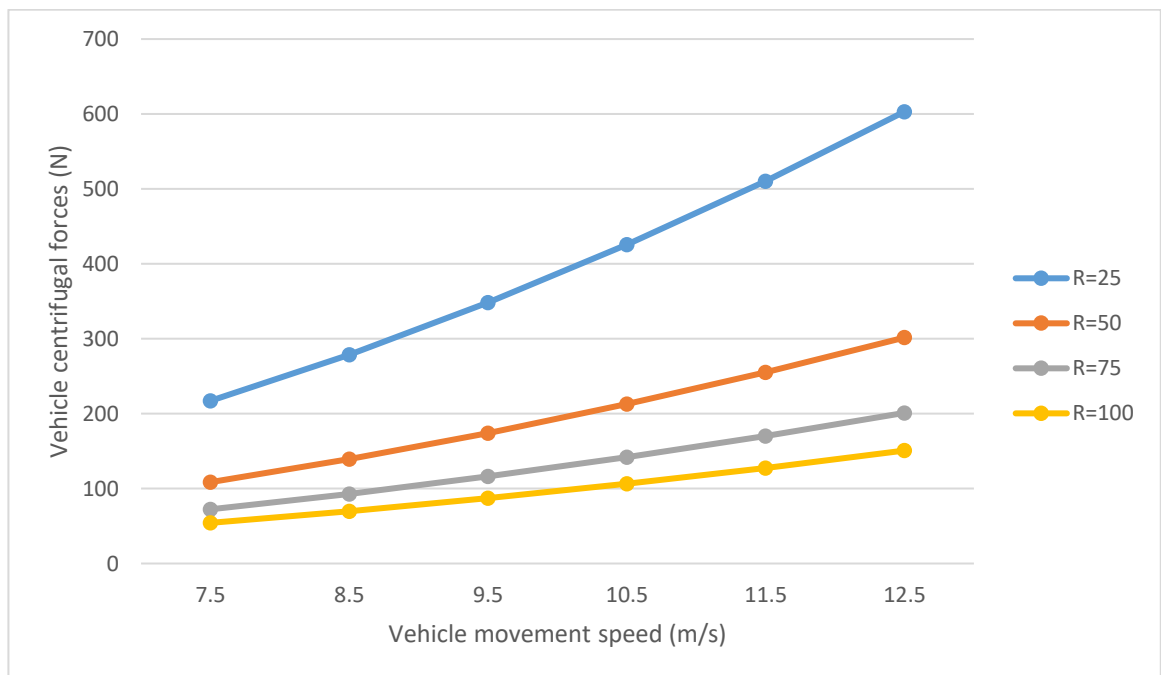


Figure 35. Centrifugal force dependence on Vehicle movement speed

The centrifugal force acting on the vehicle while cornering driving condition. The value of centrifugal force is depending on the vehicle movement speed for different turning radius. On each turning radius the centrifugal force increases with increasing of speed. Moreover, on each constant speed with increasing of turning radius the centrifugal force decreases hence the dynamic stability of vehicle increases. Dynamic stability of the vehicle decreases with higher centrifugal force and it respectively increases with lower centrifugal force.

5.13. A critical vehicle's rollover angle in the vertical longitudinal plane of the vehicle

A critical vehicle's rollover angle in the vertical longitudinal plane of the during the start-up.

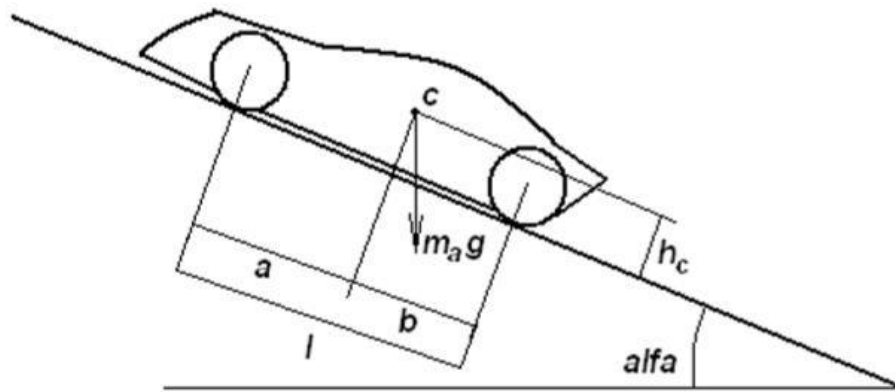


Figure 36. Critical vehicle's rollover angle [28]

$$\alpha_{kr} = \text{Arctg} \frac{b - \omega x * a \left(\frac{rd}{w}\right)}{hc} \text{ when the rear wheel drive}$$

$$\alpha_{kr} = \text{Arctg} \frac{b - \omega x * b \left(\frac{rd}{w}\right)}{hc} \text{ when the front wheel drive}$$

Tricycle is made with rear wheel drive hence, equation $\alpha_{kr} = \text{Arctg} \frac{b - \omega x * a \left(\frac{rd}{w}\right)}{hc}$ is to be used.

Where;

ωx – longitudinal wheel grip factor (for calculations accepted max grip factor $0.8 \div 0.9$, when the road surface is dry asphalt).

h_c - height of C.G. – 387.6 mm

rd - dynamic wheel radius mm – 85.95 mm

w - wheel base- 1200 mm

a - Distance of C.G. from front wheel centre

b – $(w-a)$ wheel base – distance of c.g. from front wheel centre – 107.5

$\arct=0.45 g$

$$\alpha_{kr} = 0.45 \frac{107.5 - 0.88 * 1092.5 \left(\frac{85.95}{1200} \right)}{387.6}$$

$$\alpha_{kr} = 9.64^\circ$$

5.14. Force calculation for frame FEA analysis

5.14.1. Bending Force

Total bending force = (Passenger's weight + Batteries weight)

$$\therefore (100 + 30) * 9.81 = 1275.30\text{N}$$

5.14.2. Torsion Force

Torsion Force on one side in downward direction = Total weight on frame/2) * 9.81

$$= (130/2) * 9.81 = 637.65 \text{ N}$$

Table 20. Load cases

Loading Case	Force	Unite
Bending	1275.30	N
Torsion	650	N
Lateral	50	N
Steering operational Load	50	N
Natural Frequency	N/A	

5.15. Meshing Geometry for Analysis

Programable Adaptive meshing has been selected for element mesh of the frame geometry. The Ansys program gives option of imprecise technique for meshing size.

Details of "Mesh"	
[-] Display	
Display Style	Body Color
[-] Defaults	
Physics Preference	Mechanical
<input type="checkbox"/> Relevance	0
Element Order	Program Controlled
[-] Sizing	
Size Function	Adaptive
Relevance Center	Fine
<input checked="" type="checkbox"/> Element Size	1.0 mm
Initial Size Seed	Assembly
Transition	Fast

Figure 37. Meshing properties

In manual meshing geometry could failed for element calculation as per the size and quality of mesh therefore, adaptive meshing system is best option for complex geometry meshing in Ansys program.

Adaptive Mesh tool helps to determine whether the meshing size is enough fine or not for the accurate result. If mesh size is not enough fine, adaptive mesh tool automatically re-mesh it as per the fine mesh size requirement for accurate result for particular geometry [25].

6. Result and Discussion

Result of all the analysis done with Finite Element Analysis methodology includes result of mesh element, result of bending case, torsion case, lateral case and longitudinal case. Moreover, Natural frequency, cyclic fatigue and factor of safety is also resulted for the frame FEA methodology.

6.1. Mesh result

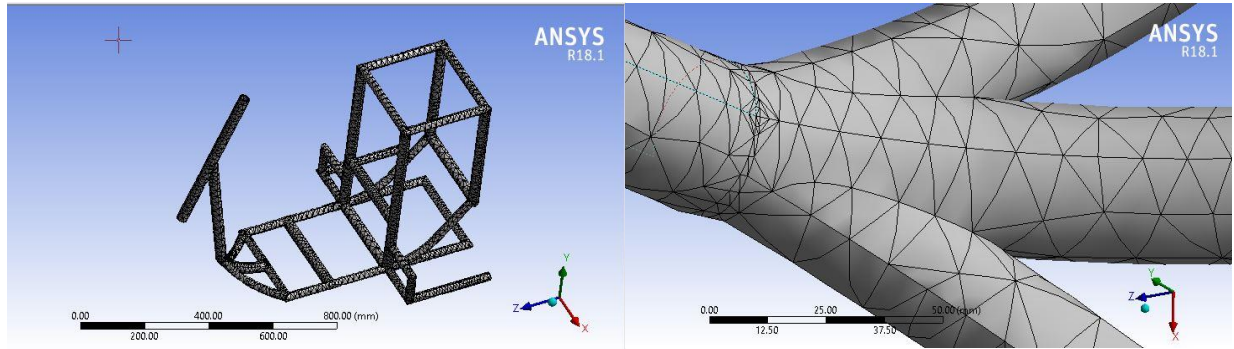


Figure 38. Mesh result

By applying programable mesh and adaptive meshing tool, fine accurate mesh is resulted as shown in the figure 38. Element size of the mesh is 1.00 mm, however where there was small section made because of edges or joining areas, adaptive mesh tool had regenerate the element mesh size enough fine so that all the analysis result will be accurate. In the zoom view of the mesh element result it is shown that joints have been meshed with different suitable fine element size and other portion of the frame has been meshed with uniformed element size by adaptive meshing tool.

6.2. Bending case

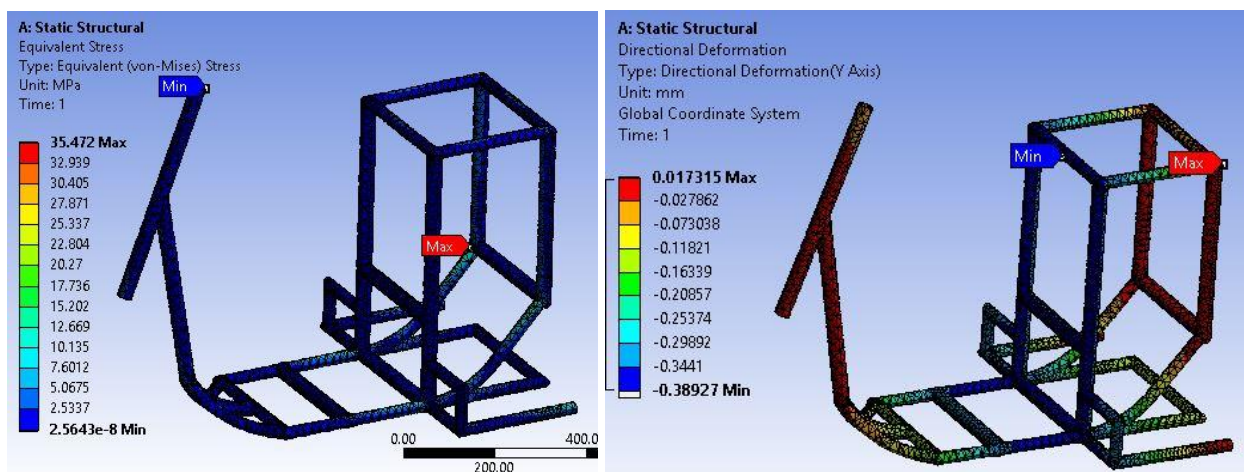


Figure 39. [a] Result of equivalent stress

[b] Result of deformation in Y axis

The stress result shown in the figure 39 [a] by applying the bending force, frame felt maximum stress of 35.472 MPa on the both joints which are connecting rear support pillar and curved pillar.

The minimum stress of 2.5×10^{-8} MPa which is almost equal to zero (negligible) is felt on the area where the steering handle connects with the bearing. The deformation result in Y axis is shown in the figure 39 [b]. The max. deformation is 0.3892mm and the minimum deformation is 0.0173. The tag of max and min shown in the figure 39 [b] should be taken as vice versa as direction of deformation is negative according to the co-ordinate system. The bending stiffness $KL = F/b$; here F-force acting on the frame, b-displacement in Y axis. So, $KL = 1275.30/0.3892 = 3276.72 \text{ N/mm} = 3.27 \text{ N/m}$

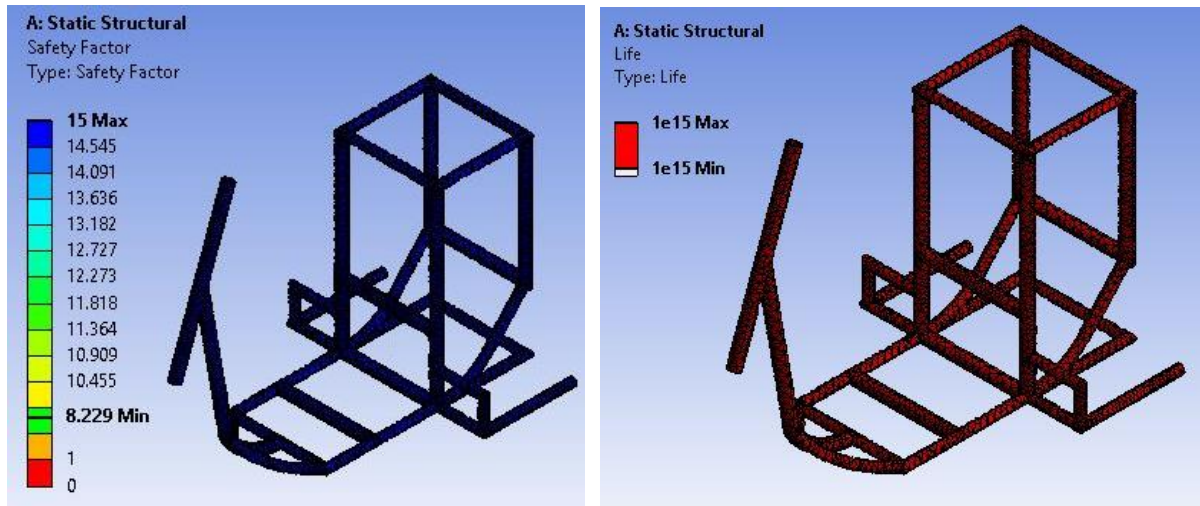


Figure 40. [a] Factor of Safety calculation [b] Result of Fatigue life

For the bending applied bending load, frame is having 15 max. factor of safety, but the minimum value is 8.229 for factor of safety which simply means design is safe enough for such bending loads. Result of fatigue analysis is 1×10^{15} cycles. The frame is permissible to perform the same bending loading operation for 1×10^{15} cycles after that it will become weaker and could not be enough strong for the same load.

6.3. Torsion case

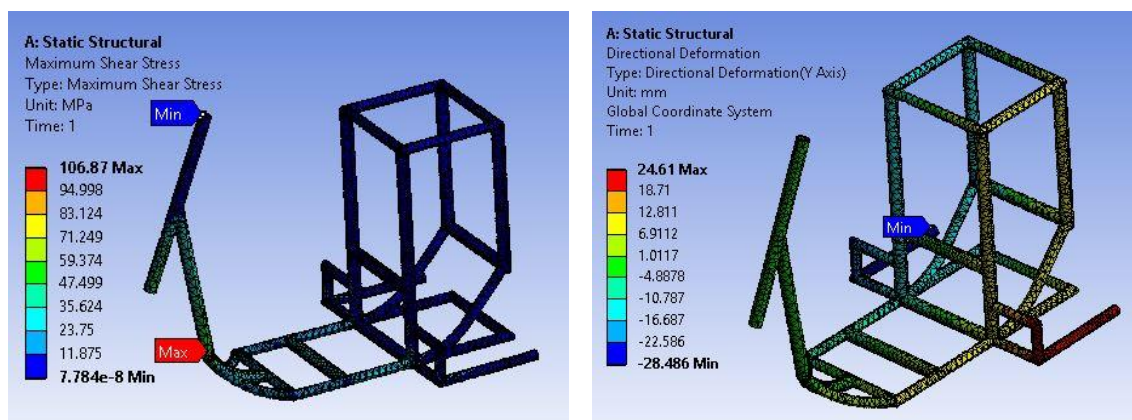


Figure 41. [a] Result of shear stress [b] Result of deformation in y axis

The result obtained by the analysis of torsion force is shown in figure 41. In figure 41 [a] max shear stress is 106.87 MPa which occurs on the joint of two pipes which is denoted by tag of max. where the min. tag shows the location where min. shear stress is occurs of 7.784×10^{-8} which is almost equal to zero hence negligible. The resultant deformation is checked in Y direction as forces acting on the y direction only. The max deformation is 28.486 mm which in upward direction and at the same time max deformation on other side is 24.61 in downward side. The tag of Min. in figure 41 shows the location of element where the max. deformation is occur and the direction is upward or positive direction. torsion rigidity $K_s = M / \alpha$; $M = F * L$; $\alpha = \arctg [b / (L/2)]$; where M-moment; α - angle a distance from the axis; b - displacement in Y axis. $L=450$ mm; $M = F*L = 650*450 = 292500$ N.mm = 292.5 N.mm; $b = 28$ mm; $\alpha = \arctg[28/ (450/2)]$; $\alpha = 7.0936^\circ$; $K_s=292.5/7.0936 =41.2339$ Nm/°.

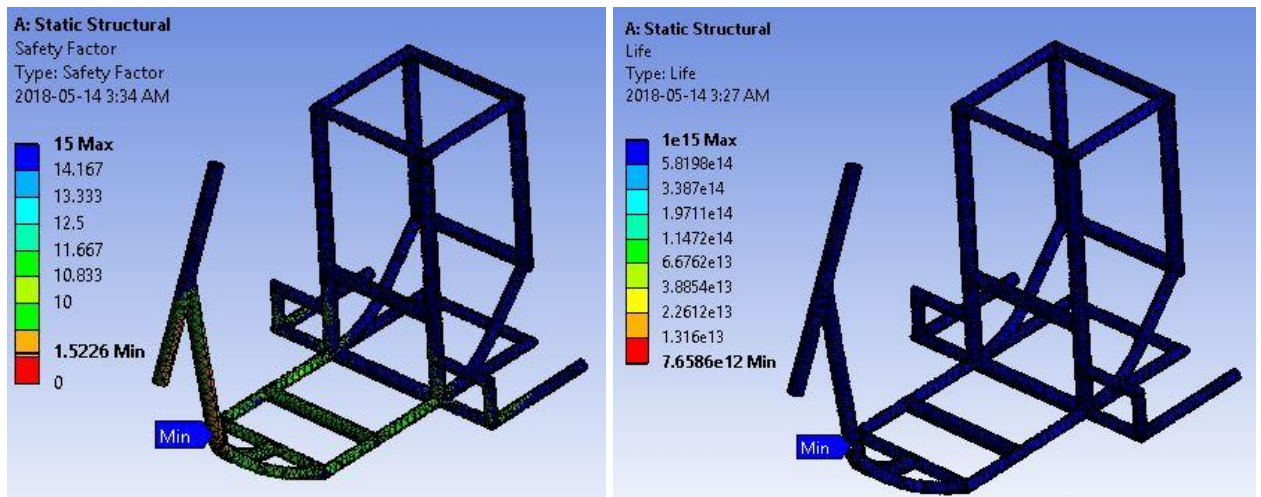


Figure 42. [a] Safety factor

[b] Result of fatigue life

Minimum factor of safety is 1.5 at the joint of two pipes which is shown in figure 6.3.2 [a], and max. is 15. However, design is safe. Result of fatigue life is also minimum on the same location which is 7.6586×10^{12} where the max. is 1×10^{15} . Minimum fatigue life area will start deforming or fracture after the min fatigue life cycle done.

6.4. Lateral Case

During the braking operation, when front brake is used to stop the vehicle, force is acting on the opposite longitudinal direction of the vehicle moving direction. The effect of the resistance force to the frame structure is analysed in lateral case. The braking force is taken in between 50N to 1000N. The braking force is varying each time depending on requirement. Thus, for critical case 1000N has been taken. Mostly working braking force would be 50N to 500N, analysis result shows for 50N and 1000N braking force. Lateral forces are directly applied to the pipe which holds steering as it is directly connected to front wheel and front brake.

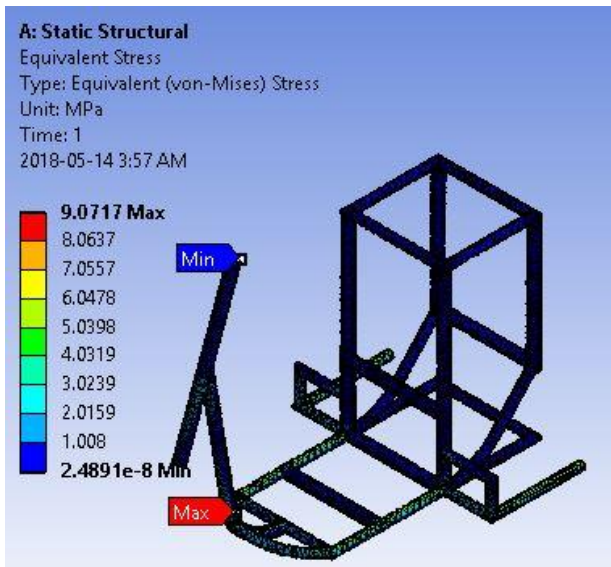
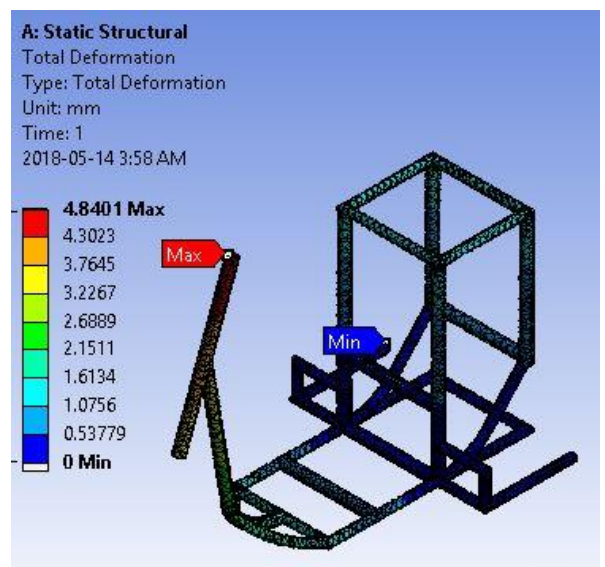


Figure 43. [a] Equivalent stress on 50N



[b] Total deformation on 50N force

On the operation of braking when force is minimum about 50N, the max. stress is 9.0717 MPa and max deformation is 4.8 mm. On the application of 1000N, the max. resultant equivalent stress is 183.18 MPa and max. deformation is 82.121 mm, though minimum factor of safety is 1.59 which takes design to be said safe.

6.5. Steering operational longitudinal load case

By steering operation, force acting on the frame structure on the pipe where steering is connected and hence effects to the strength of the frame. Analysis of the longitudinal forces gives the reaction of the frame on particular forces.

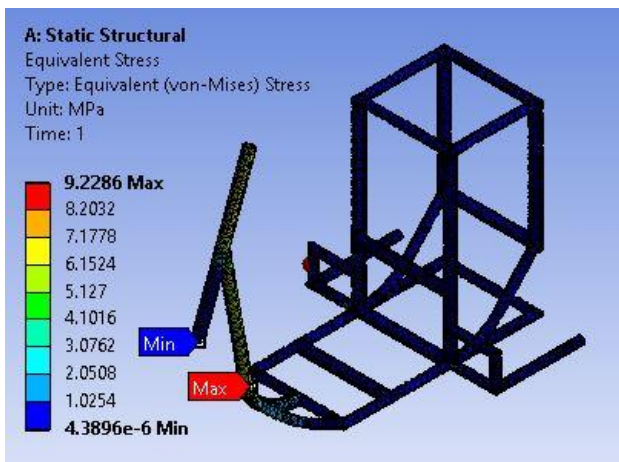
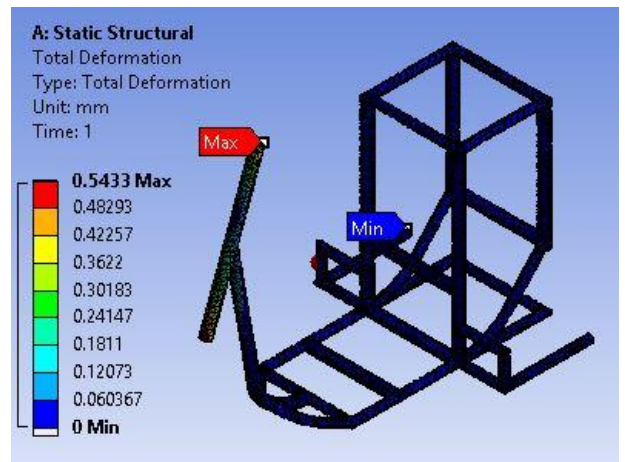


Figure 44. [a] Equivalent stress



[b] Total deformation

In the case of steering operation while considering the right turn force applied to the steering handle, which acts as a remote force on the frame structure, as a resultant max stress 9.2286 MPa occurs and minimum stress is 4.3896 MPa as shown in figure 44 [a]. The maximum deformation is 0.5433 mm and min. deformation are 0 mm. Both max. and min. deformation are shown in figure 44 [b]. For the

critical case of considering the 1000N force, the max. stress is 92.286 MPa and the max. deformation is 5.43 mm. The Yield strength of the material is 280 MPa hence, design is said to be safe for particular operation.

6.6. Natural Frequency

Natural frequency of the frame is obtained by fixing element nodes of place of all three wheels. For natural frequency there is no force applied. The analysis of natural frequency is done for 6 degrees of freedom.

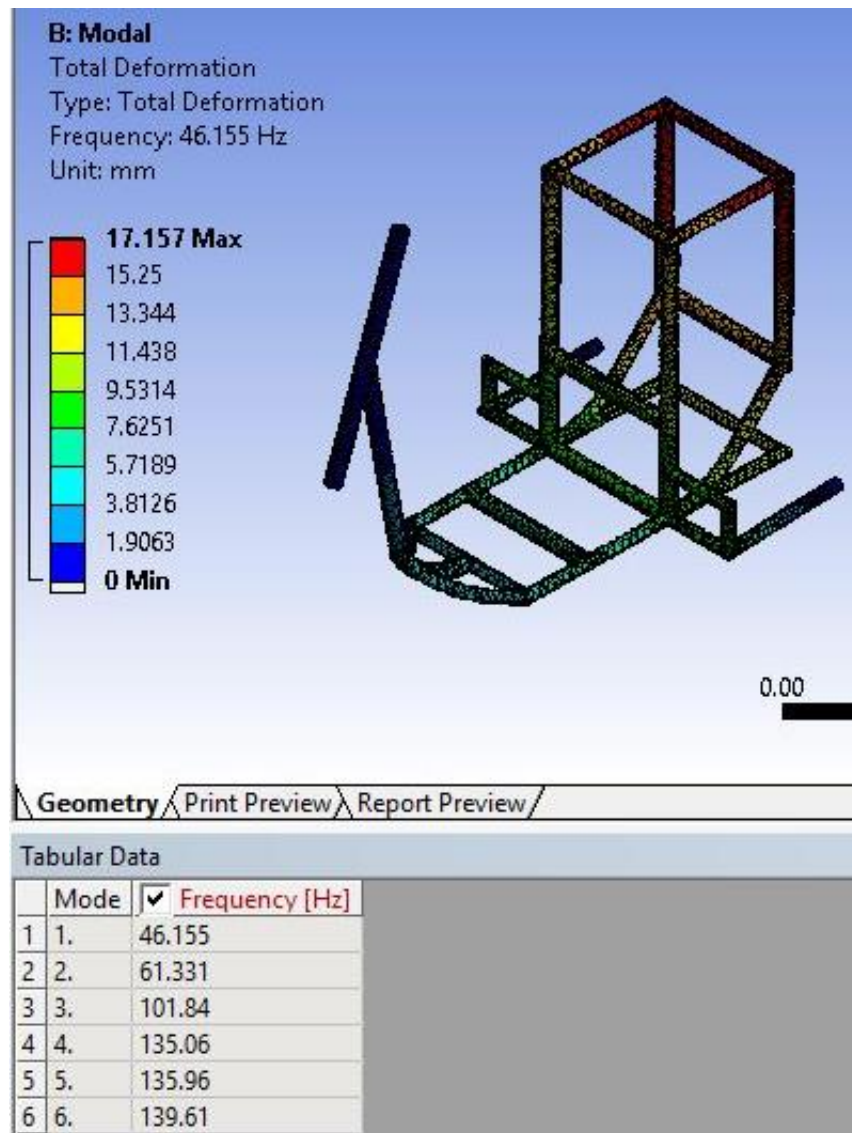


Figure 45. Natural frequencies

Result of the analysis of natural frequency is shown in the figure 45. The results are gained by 6 modes for all 6 degrees of freedom. The natural frequency could not be zero however there is no zero-natural frequency in such case. Mode 1 has 46.155 Hz, Mode 2 has 61.331 Hz, Mode 3 has 101.84 Hz, Mode 4 has 135.06 Hz, Mode 5 has 135.96 Hz and Mode 6 has 139.61 Hz frequency.

Table 21. Max. deformation on each mode (remove deformation)

Mode	Frequency [Hz]	Max. deformation
1	46.155	17.157
2	61.331	20.548
3	101.84	19.908
4	135.06	70.558
5	135.96	47.459
6	139.61	66.577

The max. deformation value for all modes is shown in table 6.6. In operational condition of the vehicle, any assembly's frequency should not match with any of these frequencies. In the case if operational frequency matches with frequency of any mode, the frame structure will deform in particular degree of freedom of that mode.

Conclusions

Identified problem is a need of alternative option of gasoline two wheelers includes bikes and mopeds as these both are the most populated vehicles in the area of study Surat city. By gaining the objectives of proposed delta type electric tricycle as a green mobility vehicle cited category of two wheelers could be replace since Delta type of tricycle has more advantage in comparison of sidecar tricycle and tadpole tricycle. CAD model of frame of tricycle has been tested with FEA methodology to check whether it is suitable and stated below.

1. The result of bending test stats max. stress on body is 35.472 MPa which is said to be safer by calculated factor of safety is 8.2.
2. The result of Torsion test stats max. shear stress on the body is 106.87 MPa which is stated as safer design by calculated factor of safety is 1.5.
3. In the case of braking operation lateral force affect very less as a resultant max. stress on the body is 9.07 MPa where the material's yield strength is 280.5 MPa.
4. In case of steering operation in longitudinal direction remote forces also doesn't leads to failure or fracture stated by felted max. stress of 9.22 MPa.
5. Natural frequencies of the part should not be zero, by the mathematical calculation of natural frequencies in ANSYS 18.1 natural frequencies of the frame have been achieved for all six degrees of freedom are 46.155 Hz, 61.331 Hz, 101.84 Hz, 135.06 Hz, 135.96 Hz and 13.61 Hz for all six modes.

Thus, it is proven that the frame is enough strong and suitable for specified such electric tricycle and such electric tricycle could replace the gasoline powered two wheelers in the area of study Surat City.

List of references

1. Integrated Mass Transit System, Surat Municipal corporation, 9th urban mobility conference and expo India 2016
2. Vehicle Populations, Commissionerate of Transport Department of Port and Transport, Government of Gujarat, Retrieved from Commissionerate of transport:
http://rtogujarat.gov.in/statistics_vehicle.php/surties.com/your-surat-on-top-with-highest-number-of-bridges/
3. Information of vehicle population, RTO Surat, Gujarat. Retrieved from RTO Surat:
https://rtosurat.gujarat.gov.in/rtosurat/CMS.aspx?content_id=5449
4. Energy and Carbon Emissions Profiles of 54 South Asian Cities, ICLEI-Local Governments for Sustainability, South Asia. Retrieved from: <http://e-lib.iclei.org/wp-content/uploads/2015/04/Energy-and-Carbon-Emissions-Profiles-for-54-South-Asian-Cities.pdf>
5. A. Rodríguez, B. Chiné, J. A. Ramírez Costa Rica Institute of Technology, School of Materials Science and Engineering, Cartago, Costa Rica, Excerpt from the Proceedings of the 2016 COMSOL Conference in Munich- 2016
6. P.P. Dutta, S. Sharma, T.K. Gogoi, R. Gogoi, K. Barman, A. Mahanta, A. Choudhury, D. Baruah, S. Gupta, A. Das- Department of Mechanical Engineering, Department of Electronics and C. Engineering, School of Engineering, Tezpur (Central) University, Assam, India, October 2013
7. Central Mechanical Engineering Research Institute data. Retrieved from: <http://www.cmeri.res.in/oth/news.htm> Accessed on 2018/05/09
8. Design and Development of a Hybrid Human Powered Vehicle by Swarnim Shrishti and Anand Amrit DEPARTMENT OF INDUSTRIAL DESIGN, NATIONAL INSTITUTE OF TECHNOLOGY, ROURKELA-769008, India-2014
9. Design, Analysis & Fabrication of Efficycle: A Hybrid Tricycle by Prof. S. U. Gunjal#1, Prof. G. D. Sonawane#2, Prof. S. P. Awate#3, Prof. D. R. Satpute#4 - Assistant Professor, Department of Mechanical Engineering Sandip Foundation's - SITRC, Mahirawani, Nashik 422213 Savitribai Phule Pune University, Pune, Maharashtra, I- International Journal of Engineering Trends and Technology (IJETT) – Volume17 Number 8–Nov2014
10. Guarnieri, M. (2012). "Looking back to electric cars". Proc. HISTELCON 2012 - 3rd Region- 8 IEEE HISTory of Electro - Technology CONference: The Origins of Electrotechnologies: #6487583.
11. Jump up^ Today in Technology History: July 6, The Center for the Study of Technology and Science, archived from the original on 2009-10-15

12. Jump up^ Sibrandus Stratingh (1785–1841), Professor of Chemistry and Technology, University of Groningen – English available
13. Electric Vehicles History Part III, electric vehicle news.com / <http://www.electricvehiclesnews.com/History/historyearlyIII.htm/> cited on 10/05/2018
14. Jetrike.Com - Tadpole or Delta?". www.jetrike.com.
15. Jump up: "Sheldon Brown's Bicycle Glossary Ta - To"
16. <https://www.pinterest.com/pin/495114552756401690/>
17. 'PM to launch mission plan for electric cars soon' Business standards, http://www.business-standard.com/article/economy-policy/pm-to-launch-mission-plan-for-electric-cars-soon-112112603007_1.html: sited on: 12-05-2018.
18. E-vehicles charging stations need no licence: The Times of India. Sited on 12-05-2018.
19. Vide S.O. 425(E), dated 9th June 1989, published in the Gazette of India, Extra., Pt. II, Sec. 3(ii), dated 9th June 1989.
20. R.T.O. Surat, Gujarat, India. https://rtosurat.gujarat.gov.in/rtosurat/CMS.aspx?content_id=5449 sited on 12-05-2018.
21. Concepts, SOLIDWORKS Fundamentals, SOLIDWORKS guide.
22. COMPARISON OF ALUMINIUM ALLOY AND STEEL MATERIALS AS DECKHOUSES FOR OFFSHORE SUPPORTVESSELS, by MuzathikA.M., FerryM., ChanM.Y., SamoK.B. and NoorC.W.M., nternational Conference on Marine TechnologyKuala Terengganu, Malaysia, 20-22 October 2012
23. Outline of general materials, Engineering Data, Workbench library.
24. Chapter 3: Adaptive Meshing, ANSYS Advanced Analysis Techniques. Retrieved from: http://www.ansys.stuba.sk/html/guide_55/g-adv/GADV3.htm
25. Tyre trax, retrieved from: <http://www.tyretrax.com/guidetoalignment.html>
26. Protean To Begin In-Wheel Electric Motor Production In 2014, GAS2, Retrieved at: <https://gas2.org/2013/04/17/protean-to-begin-in-wheel-electric-motor-production-in-2014/>
27. L. J. Clancy (1975): Aerodynamics. Pitman Publishing Limited, London
28. Reza N. Jazar. Vehicle Dynamics: Theory and Application. Springer: 2009
29. E-book, R. Makaras, A Kersys, M. Felneris, R. Kersys, D. Juodvalkis, Tecjnologija-2018.